Basic Seismology:
Some Theory and Observations

USGS
science for a changing world

- Earthquakes occur as slip across a plane in the earth.
- Any local deformation in an elastic solid stresses nearby material, which deforms in turn, stressing nearby material, and so on …
- The local stresses and strains are linked by the constitutive properties of the material.
- Consideration of basic relationships between the forces and deformations in the material (i.e., Newton's Law) leads to equations describing the propagation of seismic waves away from the energy source.
- These propagating waves cause most of the damage in earthquakes.

USGS
science for a changing world

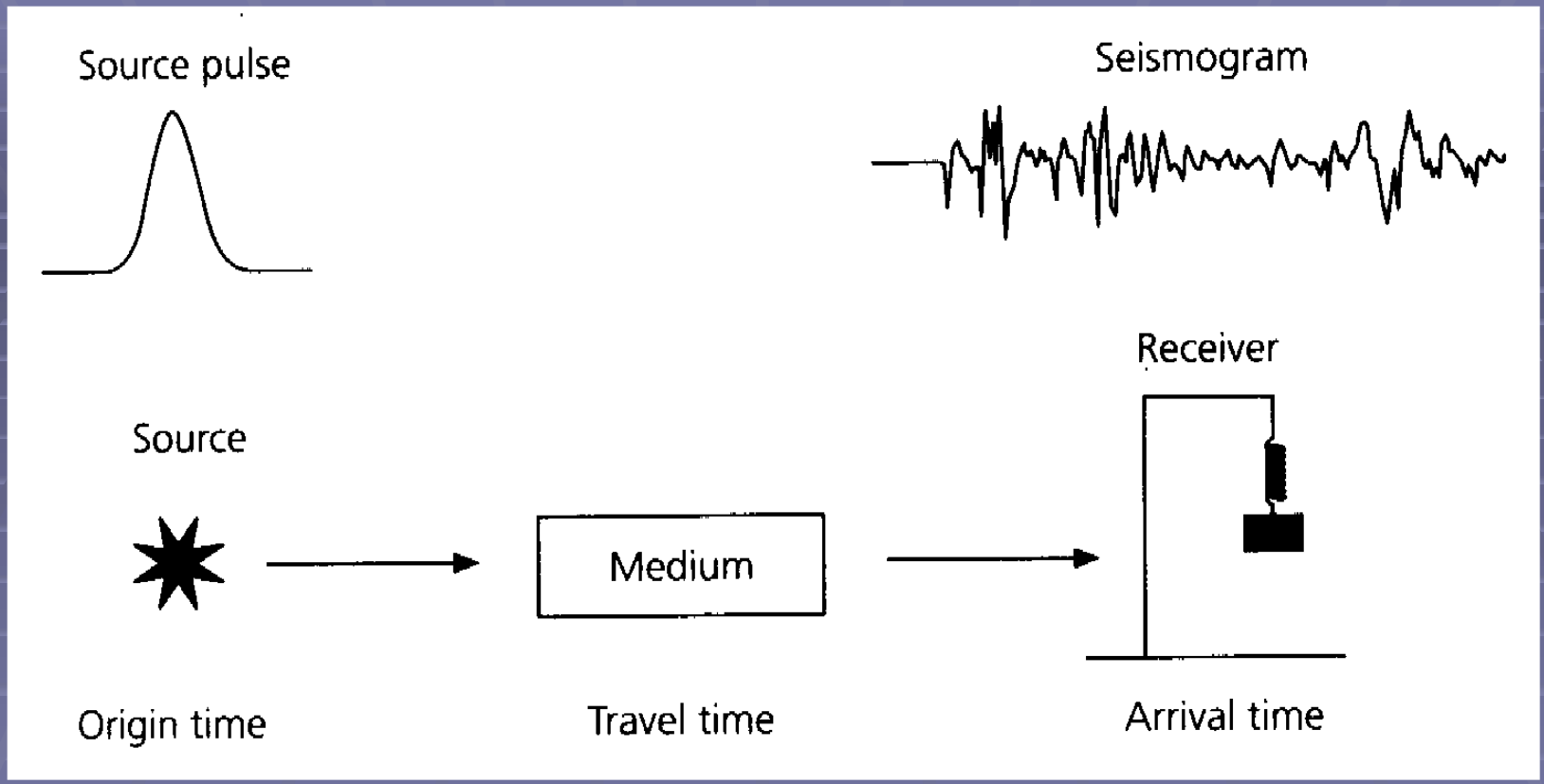

The seismic wavefield is generated at the source and modified by propagation through the earth medium where is reflected, transmitted, focused, scattered, and attenuated. Our knowledge of earthquake processes and earth structure comes from both forward modeling and inversion of earthquake travel-time and ground-shaking data.

- Shaking at a given site, say one of engineering interest, is controlled by:
  - The amount, pattern, direction, and timing of slip on the fault
  - The distance of the site from the fault
  - The types of geologic structures and materials along the wave path (e.g., waves can be focused by geologic contrasts, absorbed as they pass through materials with inefficient transmission properties, etc.)
  - The structure and physical properties of geologic materials at the site (e.g., shaking can be amplified or diminished in an alluvial basin in complex ways depending on its amplitude and frequency)

USGS
science for a changing world

CHAPTER 2

Stress and Strain

Any quantitative description of seismic wave propagation requires the ability to characterize the internal forces and deformations in solid materials. We now begin a brief review of those parts of stress and strain theory that will be needed in subsequent chapters. Although this section is intended to be self-contained, we will not derive many equations and the reader is referred to any continuum mechanics text (e.g., Malvern, 1969) for further details.

Deformations in three-dimensional materials are termed strain; internal forces between different parts of the medium are called stress. Stress and strain do not exist independently in materials; they are linked through the constitutive relationships that describe the nature of elastic solids.

2.1 The Stress Tensor

Consider an infinitesimal plane of arbitrary orientation within a homogenous elastic medium in static equilibrium. The orientation of the plane may be specified by its unit normal vector, $\hat{\mathbf{n}}$. The force per unit area exerted by the side in the direction of $\hat{\mathbf{n}}$ across this plane is termed the *traction* and is represented by the vector $\mathbf{t}(\hat{\mathbf{n}}) = (t_x, t_y, t_z)$. There is an equal and opposite force exerted by the side opposing $\hat{\mathbf{n}}$, such that $\mathbf{t}(-\hat{\mathbf{n}}) = -\mathbf{t}(\hat{\mathbf{n}})$. The part of $\mathbf{t}$ that is normal to the plane is termed the *normal stress*; that parallel to it is called the *shear stress*. In the case of a fluid, there are no shear stresses and $\mathbf{t} = -P\hat{\mathbf{n}}$, where P is the pressure.

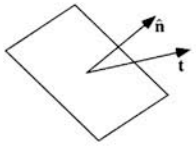

The stress tensor, $\boldsymbol{\tau}$, in a Cartesian coordinate system (Fig. 2.1) may be defined† by the tractions across the yz, xz, and xy planes:

$$\boldsymbol{\tau} = \begin{bmatrix} t_x(\hat{\mathbf{x}}) & t_x(\hat{\mathbf{y}}) & t_x(\hat{\mathbf{z}}) \\ t_y(\hat{\mathbf{x}}) & t_y(\hat{\mathbf{y}}) & t_y(\hat{\mathbf{z}}) \\ t_z(\hat{\mathbf{x}}) & t_z(\hat{\mathbf{y}}) & t_z(\hat{\mathbf{z}}) \end{bmatrix} = \begin{bmatrix} \tau_{xx} & \tau_{xy} & \tau_{xz} \\ \tau_{yx} & \tau_{yy} & \tau_{yz} \\ \tau_{zx} & \tau_{zy} & \tau_{zz} \end{bmatrix}. \qquad (2.1)$$

Development of the seismic wave equation begins with consideration of the forces acting on an infinitesimal plane within a homogeneous elastic medium in static equilibrium.

Forces (stress) and deformation (strain) at a point in a general elastic solid are related by a (81-component) fourth-order constitutive tensor. If the physical properties of the medium are direction-independent (isotropic), a good first-order approximation for the earth, the number of independent elastic parameters reduces to two. The P-wave and S-wave seismic velocities at each point in the medium can be determined from these two elastic parameters and the density.

"Introduction To Seismology" by P. Shearer, Cambridge University Press

USGS science for a changing world

CHAPTER 3

The Seismic Wave Equation

Using the stress and strain theory developed in the previous chapter, we now construct and solve the seismic wave equation for elastic wave propagation in a uniform whole space. This chapter will involve vector calculus and complex numbers; some of the mathematics is reviewed in Appendix 2.

3.1 The Momentum Equation

In the previous chapter, the stress, strain, and displacement fields were considered in static equilibrium and unchanging with time. However, because seismic waves are time-dependent phenomena that involve velocities and accelerations, we need to account for the effect of momentum. We do this by applying Newton's law ($F = ma$ from your freshman physics class) to a continuous medium.

Consider the forces on an infinitesimal cube in a (x_1, x_2, x_3) coordinate system (Fig. 3.1). The forces on each surface of the cube are given by the product of the traction vector and the surface area. For example, the force on the plane normal to x_1 is given by

$$\begin{aligned}\mathbf{F}(\hat{\mathbf{x}}_1) &= \mathbf{t}(\hat{\mathbf{x}}_1)\, dx_2\, dx_3 \\ &= \boldsymbol{\tau}\hat{\mathbf{x}}_1\, dx_2\, dx_3 \\ &= \begin{bmatrix} \tau_{11} \\ \tau_{21} \\ \tau_{31} \end{bmatrix} dx_2\, dx_3, \end{aligned} \tag{3.1}$$

where $\mathbf{F}$ is the force vector, $\mathbf{t}$ is the traction vector, and $\boldsymbol{\tau}$ is the stress tensor. In the case of a homogeneous stress field, there is no net force on the cube since the forces on opposing sides will cancel out, that is, $\mathbf{F}(-\hat{\mathbf{x}}_1) = -\mathbf{F}(\hat{\mathbf{x}}_1)$. Net force will only be exerted on the cube if spatial gradients are present in the stress field. In this case, the net force from the planes normal to x_1 is

$$\mathbf{F}(\hat{\mathbf{x}}_1) = \frac{\partial}{\partial x_1} \begin{bmatrix} \tau_{11} \\ \tau_{21} \\ \tau_{31} \end{bmatrix} dx_1\, dx_2\, dx_3, \tag{3.2}$$

Now consider an infinitesimal cube embedded within a homogeneous, isotropic elastic medium. If the stress field is homogeneous there is no net force on the cube, but spatial gradients in the stress field generate net forces. The cube is now in motion, and we use Newton's Law to derive the equation of motion.

We can use relationships between stress and strain to express stress gradients in terms of displacements. These equations can be used directly in finite-difference equations. Otherwise, we can use vector calculus to derive simpler wave equations for the P-wave and S-wave fields.

"Introduction To Seismology" by P. Shearer, Cambridge University Press

USGS science for a changing world

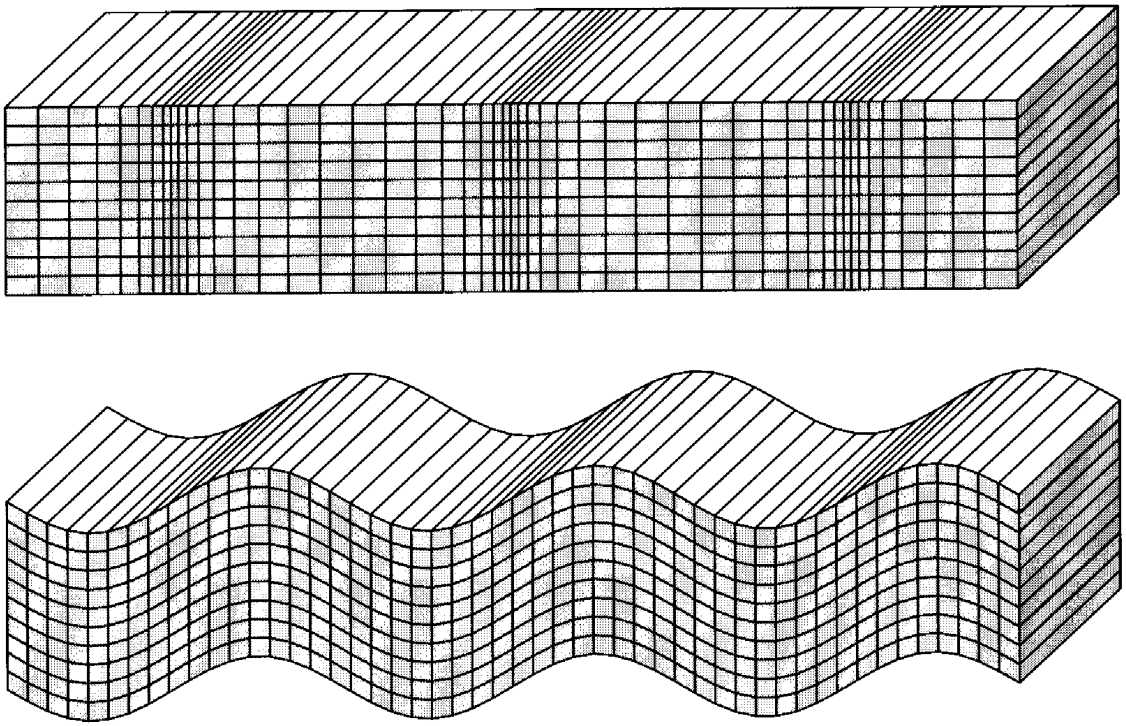

Fig. 3.2. Displacements occurring from a harmonic plane P-wave (top) and S-wave (bottom) traveling horizontally across the page. S-wave propagation is pure shear with no volume change, whereas P-waves involve both a volume change and shearing (change in shape) in the material. Strains are highly exaggerated compared to actual seismic strains in the Earth.

$$\mathbf{u}(\mathbf{x}, t) = \mathbf{A}(\omega)e^{-i\omega(t-\mathbf{s}\cdot\mathbf{x})}$$
$$= \mathbf{A}(\omega)e^{-i(\omega t-\mathbf{k}\cdot\mathbf{x})},$$

Real seismic wavefronts in the earth are curved, but a plane wave can be a useful concept. (For example, a spherical wave can be expressed as a sum of plane waves.) This is the general form of a plane wave in the frequency domain. Displacement varies in time and space (x-dimension only in this case), expressed as an amplitude term times a harmonic function of frequency and slowness, *s*, or wavenumber, *k*. A spherical wave has a similar functional form with an additional distance decay factor of 1/r.

"Introduction To Seismology" by P. Shearer, Cambridge University Press

USGS science for a changing world

Solving The Seismic Wave Equation

Solutions of the seismic wave equation for compressional- (P-) and shear (S-) waves in a uniform whole space are readily found, but this case is not very interesting to a seismologist who is trying to model seismic waves in a realistic earth.

Interesting (non-trivial) earth models that we might wish to use contain gradients in the physical parameters that control wave propagation, but these factors severely complicate solutions of the wave equation. Several approaches have been devised that allow us to ignore the gradient terms and find an approximate solution, yet still include some realistic structure in the model.

Homogeneous Layer Methods

- To first order, seismic velocity is a function only of depth in the earth; the earth can be modeled as a series of homogeneous layers in which the gradient terms vanish.
- Wave propagation inside each layer is simple; it only remains to keep track of interactions of the wave field (reflection and transmission) at the layer boundaries (this is a simpler problem).
- A continuous 1-dimensional velocity gradient can be modeled by simply increasing the number of layers.

Ray Methods

- The importance of the gradient terms varies as 1/frequency, so they become vanishingly small for high-frequency waves. Thus, rays traced through a model with continuous physical properties accurately describe the high-frequency wave field.

CHAPTER 4

Ray Theory: Travel Times

Seismic ray theory is analogous to optical ray theory and has been applied for over 100 years to interpret seismic data. It continues to be used extensively today, due to its simplicity and applicability to a wide range of problems. These applications include most earthquake location algorithms, body wave focal mechanism determinations, and inversions for velocity structure in the crust and mantle. Ray theory is intuitively easy to understand, simple to program, and very efficient. Compared to more complete solutions, it is relatively straightforward to generalize to three-dimensional velocity models. However, ray theory also has several important limitations. It is a high-frequency approximation, which may fail at long periods or within steep velocity gradients, and it does not easily predict any "nongeometrical" effects, such as head waves or diffracted waves. The ray geometries must be completely specified, making it difficult to study the effects of reverberation and resonance due to multiple reflections within a layer.

In this chapter, we will be concerned only with the timing of seismic arrivals, deferring the consideration of amplitudes and other details to later. This narrow focus is nonetheless very useful for many problems; a significant fraction of current research in seismology uses only travel time information. The theoretical basis for much of ray theory is derived from the *eikonal equation* (see Appendix 3); however, because these results are not required for most applications we do not describe them here.

4.1 Snell's Law

Consider a plane wave, propagating in material of uniform velocity v, that intersects a horizontal interface (Fig. 4.1). The wavefronts at time t and time $t + \Delta t$ are separated by a distance Δs along the ray path. The ray angle from the vertical, θ, is termed the incidence angle. This angle relates Δs to the wavefront separation on the interface, Δx, by

$$\Delta s = \Delta x \sin\theta. \tag{4.1}$$

Since $\Delta s = v\Delta t$, we have

$$v\Delta t = \Delta x \sin\theta \tag{4.2}$$

Ray Theory

- A high-frequency approximation
- Simple to program, computationally efficient, and easy to generalize to 3-dimensional earth models
- Good for: modeling seismic phase arrival times, earthquake location algorithms, body-wave focal mechanism determinations, inversions for velocity structure
- Not very good for: amplitudes because it is a high-frequency approximation

"Introduction To Seismology" by P. Shearer, Cambridge University Press

USGS science for a changing world

4.2 Ray Paths for Laterally Homogeneous Models

In most cases the compressional and shear velocities increase as a function of depth in the Earth. Suppose we examine a ray traveling downward through a series of layers, each of which is faster than the layer above. The ray parameter p remains constant and we have

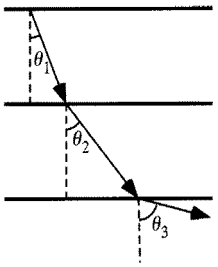

$$p = u_1 \sin\theta_1 = u_2 \sin\theta_2 = u_3 \sin\theta_3. \qquad (4.5)$$

If the velocity continues to increase, θ will eventually equal 90° and the ray will be traveling horizontally.

This is also true for continuous velocity gradients (Fig. 4.3). If we let the slowness at the surface be u_0 and the *takeoff angle* be θ_0, we have

$$u_0 \sin\theta_0 = p = u \sin\theta. \qquad (4.6)$$

When $\theta = 90°$ we say that the ray is at its *turning point* and $p = u_{tp}$, where u_{tp} is the slowness at the turning point. Since velocity generally increases with depth in Earth, the slowness *decreases* with depth. Smaller ray parameters are more steeply dipping at the surface, will turn deeper in Earth, and generally travel farther. In these examples with horizontal layers or vertical velocity gradients, p remains constant along the ray path. However, if lateral velocity gradients or dipping layers are present, then p will change along the ray path.

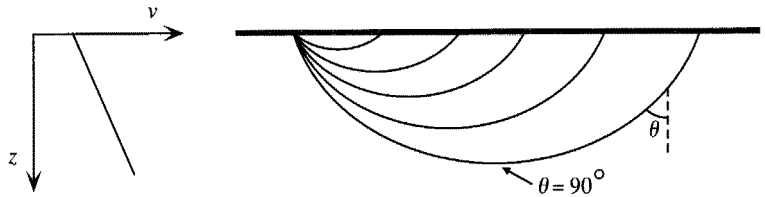

Fig. 4.3. Ray paths for a model with a continuous velocity increase with depth will curve back toward the surface. The ray turning point is defined as the lowermost point on the ray path, where the ray direction is horizontal and the incidence angle is 90°.

A seismic version of Snell's Law from optics can be used to track ray geometry through inhomogeneous materials. Rays can be traced through regions with continuous velocity gradients.

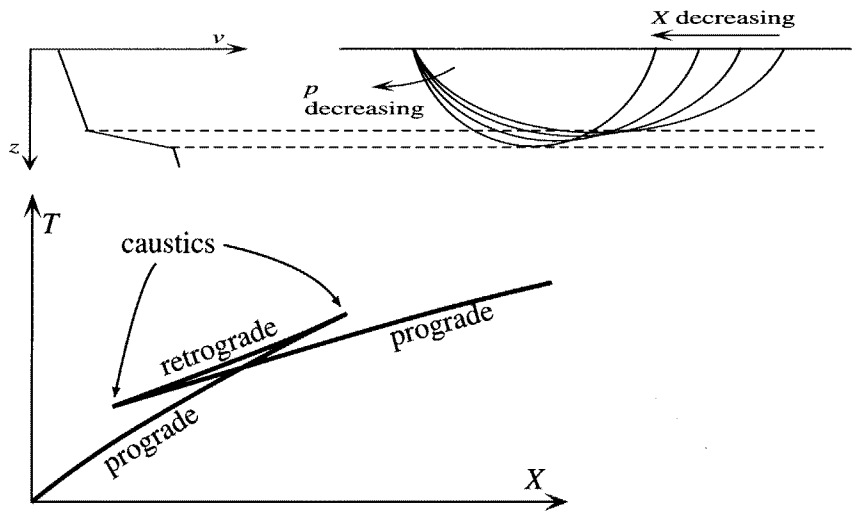

Fig. 4.5. A triplication in a travel time curve resulting from a steep velocity increase.

Ray tracing results are often summarized as travel-time curves: travel-time as a function of distance from the ray source. Each point on the curve represents a different ray path through the model. This example shows a case with a steep velocity increase. Locally a flat earth model can be used; for global studies we use a spherical earth model.

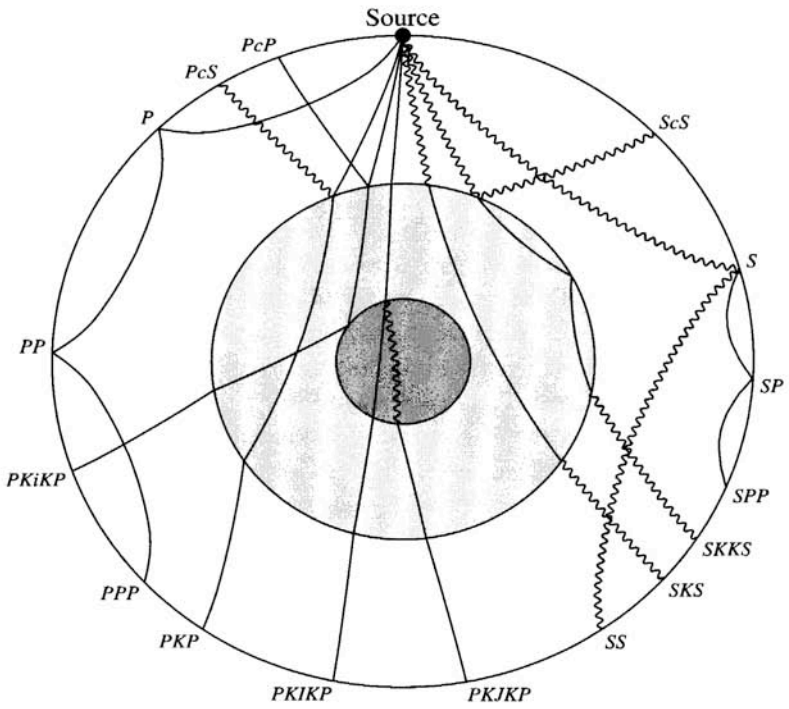

Fig. 4.14. Global seismic ray paths and phase names, computed for the PREM velocity model. *P*-waves are shown as solid lines, *S*-waves as wiggly lines. The different shades indicate the inner core, the outer core, and the mantle.

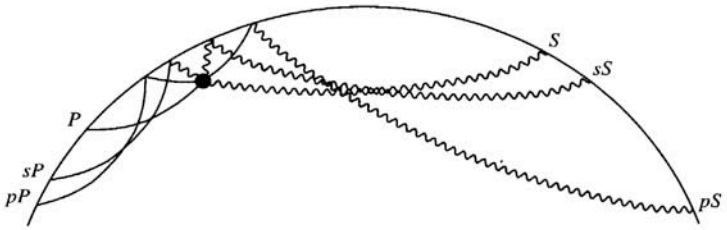

Fig. 4.15. Deep earthquakes generate surface-reflected arrivals, termed depth phases, with the upgoing leg from the source labeled with a lower-case *p* or *s*. Ray paths plotted here are for an earthquake at 650 km depth, using the PREM velocity model.

Rays are a particularly useful tool for studying global body-waves. This model of the earth shows the mantle, liquid outer core, and solid inner core.

Naming codes for whole-earth phases:
P: P-wave in mantle
K: P-wave in outer core
I: P-wave in inner core
S: S-wave in mantle
J: S-wave in inner core
c: reflection off core-mantle boundary
i: reflection off inner-core boundary

"Introduction To Seismology" by P. Shearer, Cambridge University Press

USGS science for a changing world

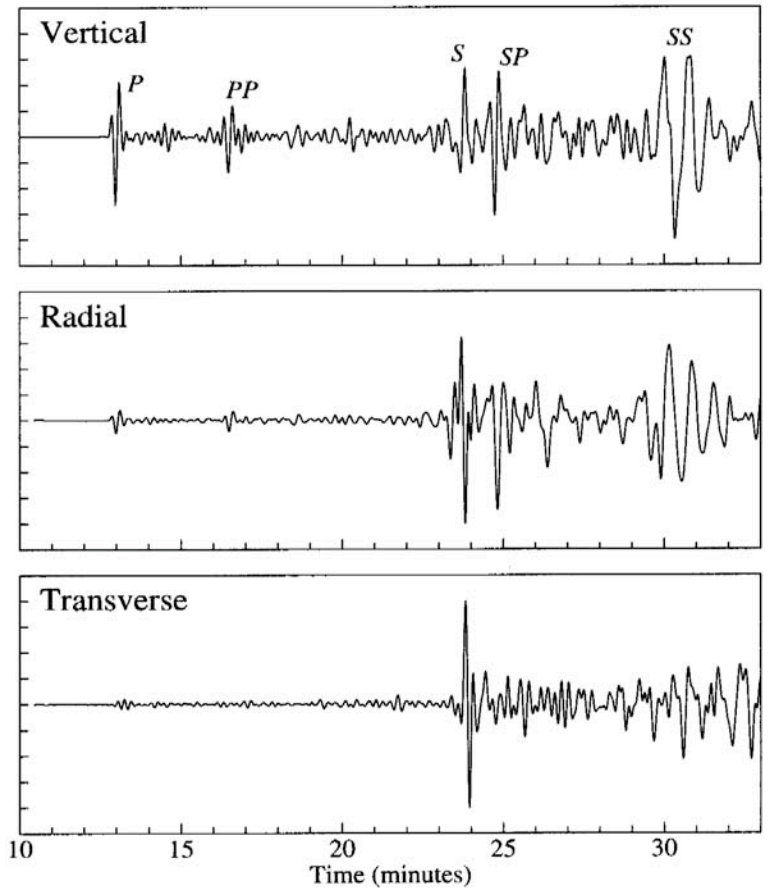

Fig. 4.16. The vertical, radial, and transverse components of ground motion (velocity) from the January 17, 1994 Northridge earthquake recorded at the IRIS/IDA station OBN at 88.5° range. The original broadband records have been filtered to between 15 and 100 s period. Time is in minutes relative to the earthquake origin time; amplitudes are self-scaled.

Seismograms are records of earthquake ground shaking vs time. Modern seismographs record three orthogonal components of ground shaking: one vertical component and two horizontal components. Ground shaking in any direction can be computed by combining these three components. To understand earth structure and earthquake processes we need records of ground shaking from a wide range of earthquake magnitudes at a wide range of distances.

"Introduction To Seismology" by P. Shearer, Cambridge University Press

USGS science for a changing world

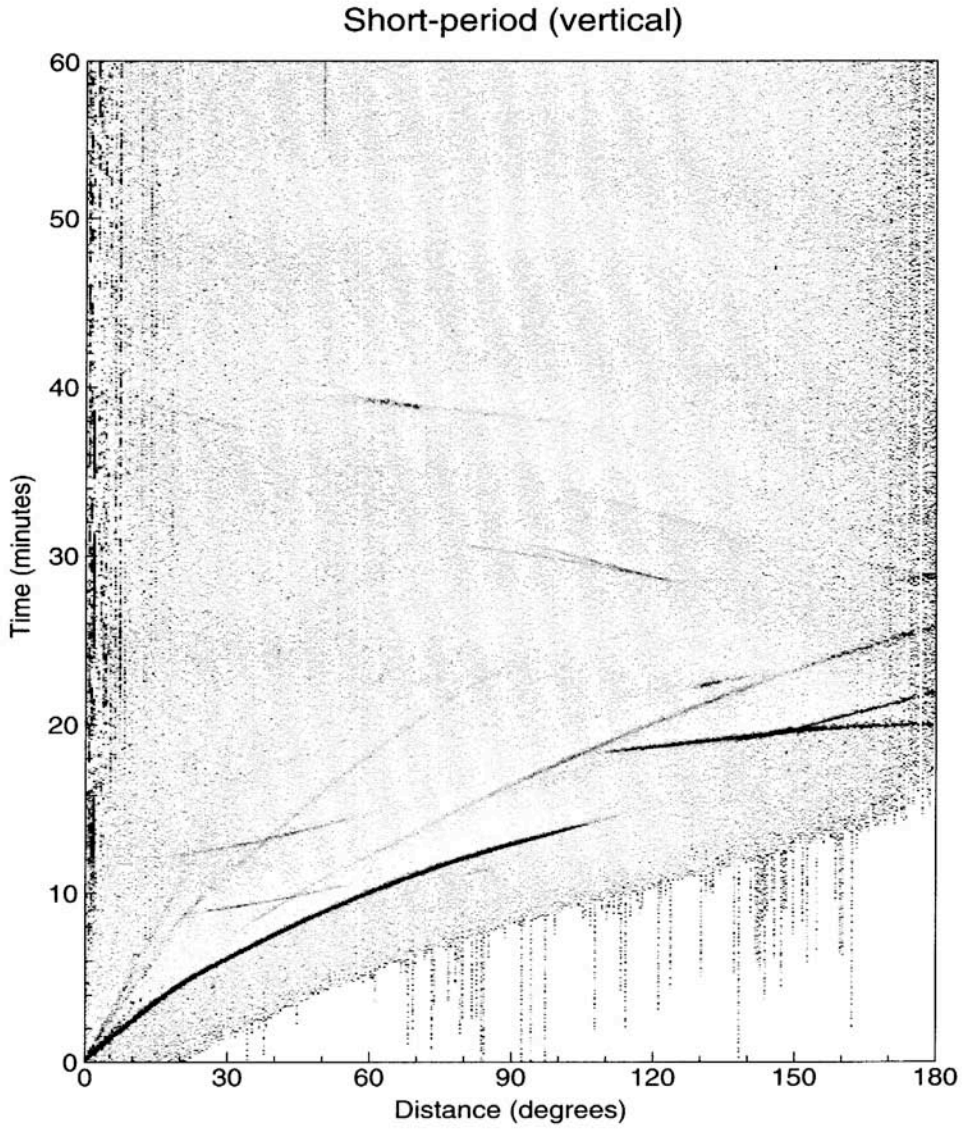

Fig. 4.18. A stack of short-period (<2 s), vertical component data from the global networks between 1988 to 1994. See Figure 4.19 for a key to the phase names. (From Astiz et al., 1996.)

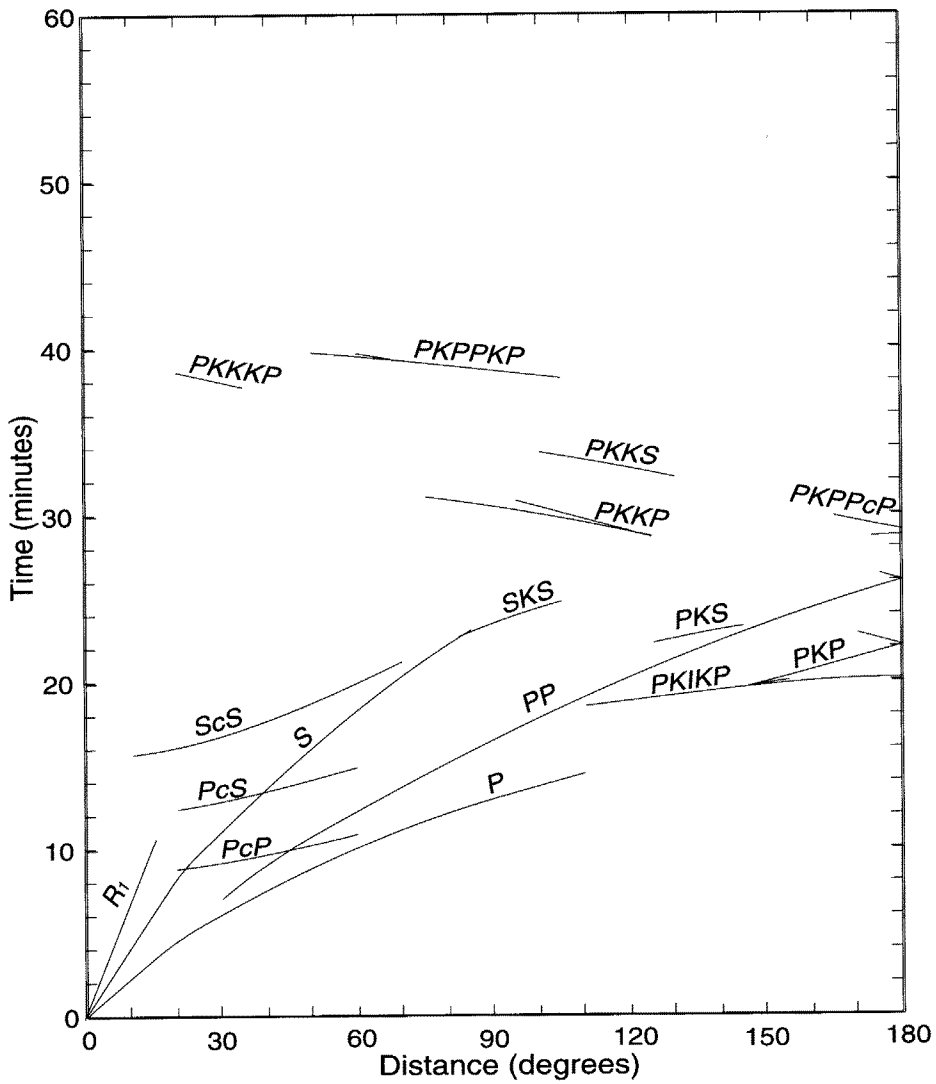

Fig. 4.19. A key to the phases visible in the short-period stack plotted in Fig. 4.18. Travel time curves are calculated using the IASP91 velocity model (Kennett and Engdahl, 1991). (From Astiz et al., 1996.)

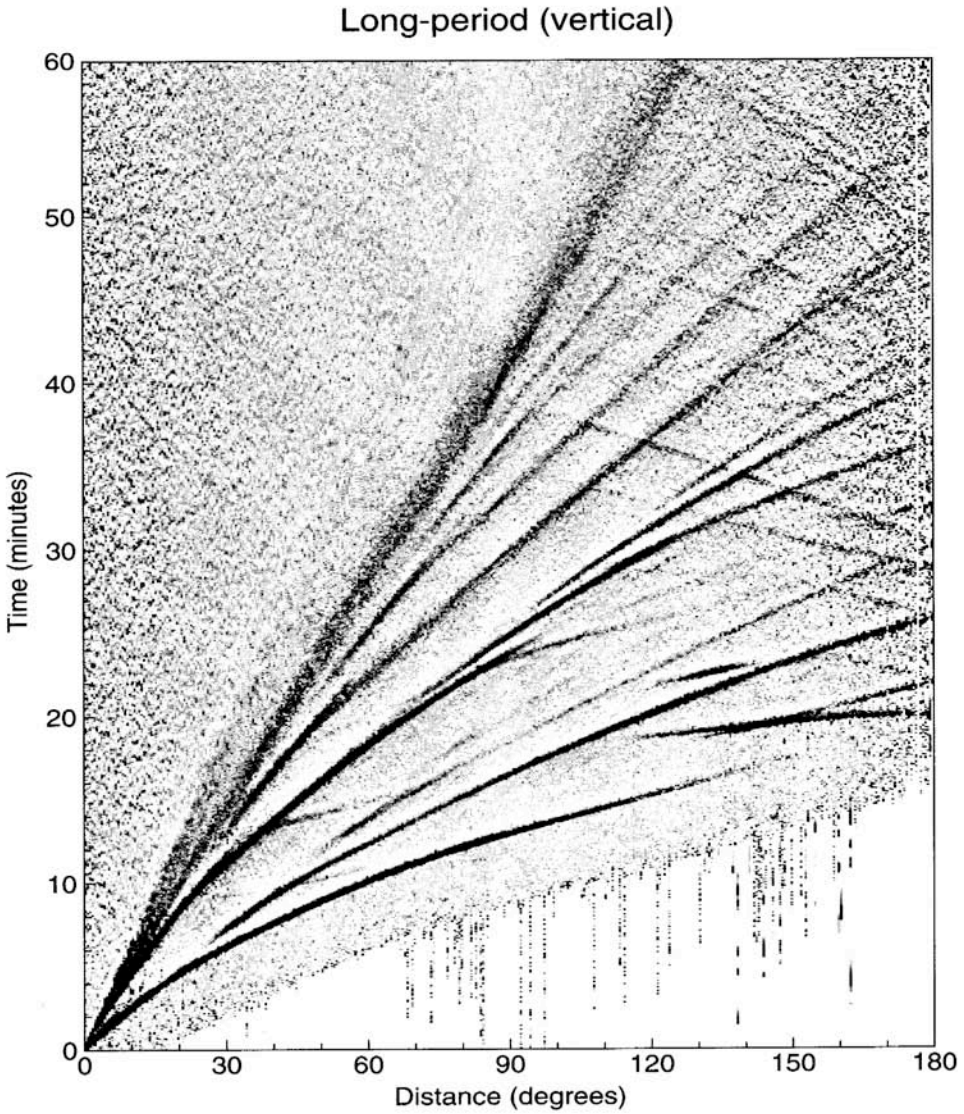

Fig. 4.20. A stack of long-period (>10 s), vertical component data from the global networks between 1988 to 1994. See Figure 4.23 for a key to the phase names. (From Astiz et al., 1996.)

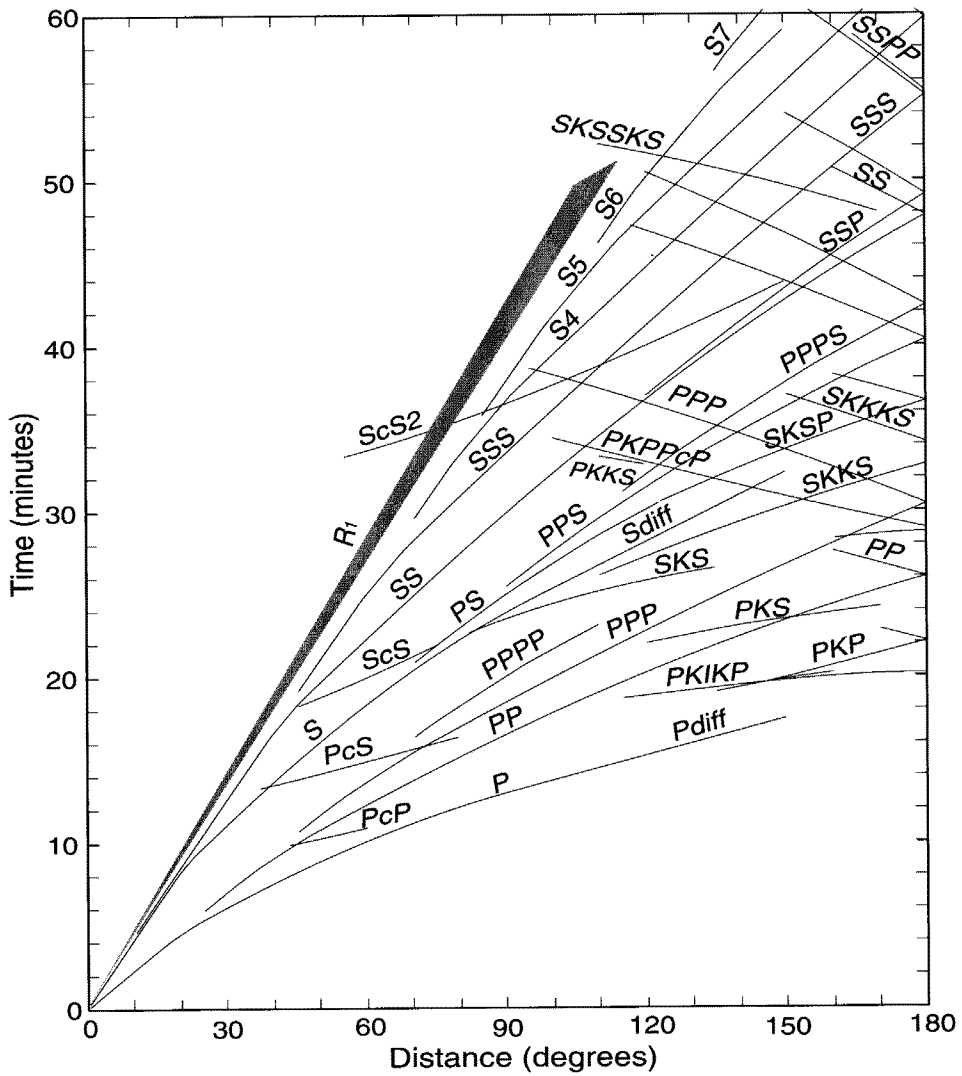

Fig. 4.23. The phases visible in the long-period stacks shown in Figures 4.20–4.22. Travel time curves are calculated using the IASP91 velocity model (Kennett and Engdahl, 1991). (From Astiz et al., 1996.)

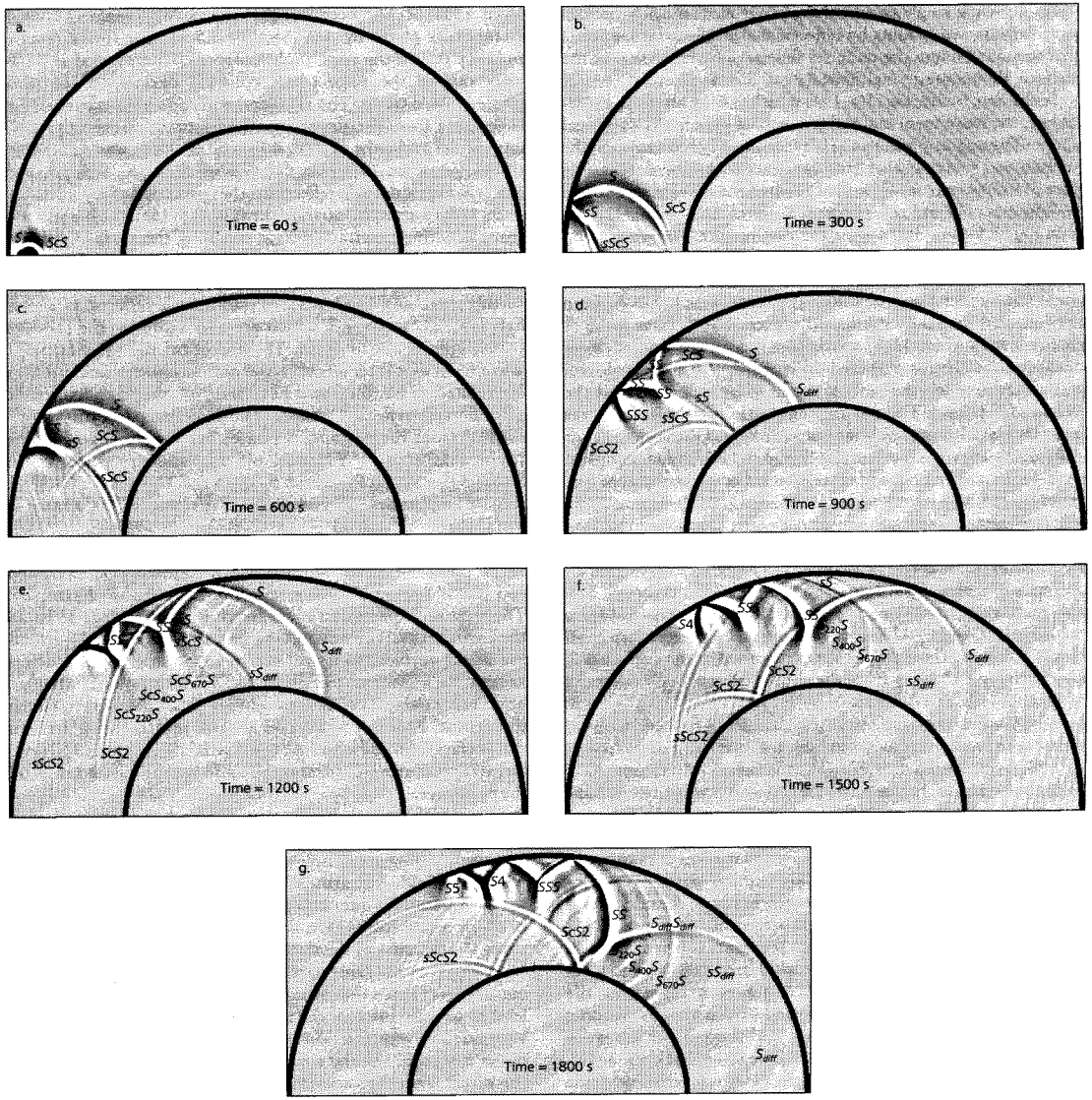

Fig. 3.5-19 Snapshots of a synthetic *SH* wave field showing the propagation of waves after a 600 km-deep earthquake. The initial wave front moves away from the source at the lower left side of the figures. The wave front develops complexity due to interactions with the surface, CMB, and internal discontinuities and velocity gradients. The wave field is computed using the spherically symmetric PREM velocity model. Amplitudes are raised to a power of 0.8 to enhance smaller signals. (After Wysession and Shore, 1994.)

CHAPTER 5

Inversion of Travel Time Data

In the preceding chapter we examined the problem of tracing rays and calculating travel time curves from a known velocity structure. We derived expressions for ray tracing in a one-dimensional (1-D) velocity model in which velocity varies only with depth; ray tracing in general three-dimensional (3-D) structures is more complex but follows similar principles. We now examine the case where we are given travel times obtained from observations and wish to invert for a velocity structure that can explain the data. As one might imagine, the inversion is much more complicated than the forward problem. The main strategy used by seismologists, both in global and crustal studies, has generally been to divide the problem into two parts:

(1) A 1-D "average" velocity model is determined from all the available data. This is generally a nonlinear problem but is tractable since we are seeking a single function of depth. Analysis often does not proceed beyond this point.
(2) If sufficient 3-D ray coverage is present, the 1-D model is used as a reference model and a travel time residual is computed for each datum by subtracting the predicted time from the observed time. A 3-D model is obtained by inverting the travel time residuals for velocity perturbations relative to the reference model. If the velocity perturbations are fairly small, this problem can be linearized and is computationally feasible even for large data sets. This is the basis for *tomographic* inversion techniques.

We now consider each of these problems in turn. For now we will assume that the source locations are precisely known, deferring discussion of the earthquake location problem to the end of the chapter.

5.1 One-Dimensional Velocity Inversion

Before beginning it is useful to imagine how one might obtain a 1-D velocity structure from travel times. Assume that we are given a simple travel time curve without any triplications or low-velocity zones. Each point on the $T(X)$ curve has a slope, which gives the velocity at the turning point of the ray. Thus, we know that a particular velocity must be present; the problem is to determine where. This is equivalent to assigning a depth to each point along the travel time curve. To do this we need to know the velocity structure above the depth in question, and so

Given travel-time observations, can we find an earth velocity structure that is consistent with the data?

Typical strategy:

1) Find an average 1-D velocity-depth function. This is a nonlinear problem, but tractable since we seek a single function of depth.
2) If enough data are available we can get a 3 -D model from travel-time residuals relative to a 1-D reference model (seismic tomography).

"Introduction To Seismology" by P. Shearer, Cambridge University Press

USGS science for a changing world

Elegant integral-transform methods (e.g., Herglotz-Wiechert) have been developed to derive 1-D velocity models, but it can be difficult to apply formal inversions to noisy and/or discontinuous travel-time data. A simple alternative is to fit the travel-time data with a series of straight segments. Each segment corresponds to a homogeneous layer in the model.

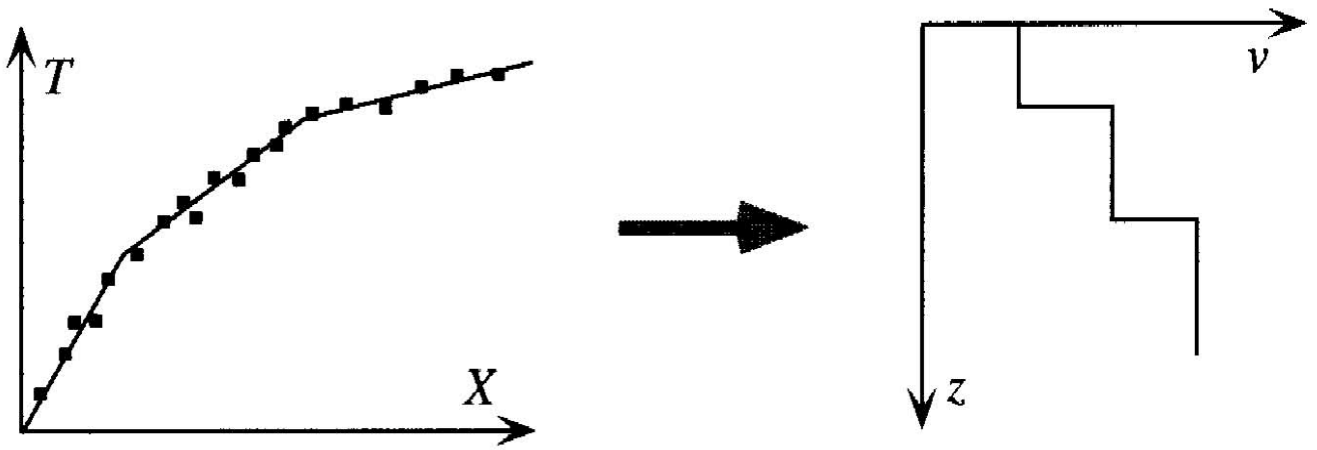

Fig. 5.2. Straight lines fit to $T(X)$ data can be inverted for a "layer cake" velocity model.

Variable changes and other mathematical tricks can be used to linearize the problem and simplify the inversion. However …

It's not clear that it pays to push 1-D travel-time inversion methods much further. For example, seismograms contain more information than travel-times alone (amplitudes are very sensitive to velocity gradients) and are now readily available in digital form.

The current state of the art involves synthetic seismogram modeling of the entire waveform, and seismic tomography, 3-D inversions of large datasets of travel-time residuals (differences between observed and predicted travel-times).

Seismic Tomography

Assuming that a reference 1-D model is available, the next step is to parameterize the model of 3-D velocity perturbations. This is commonly done in two different ways: (1) the model is divided into blocks of uniform velocity perturbation or (2) spherical harmonic functions can be used in the case of global models to parameterize lateral velocity perturbations, with either layers or polynomial functions used to describe vertical variations.

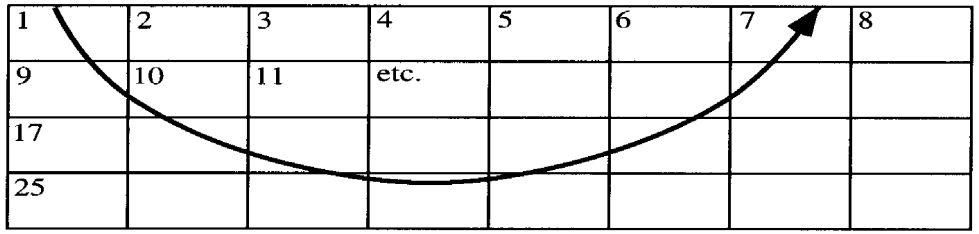

Each observed travel-time residual corresponds to a ray path that connects the source and reciever. This geometry must be determined for each observation, and then the travel-time through each block computed for each ray (this is computationally intensive). Each travel-time residual (one for each ray) can be expressed as a sum over all the blocks along the ray of the product of block travel-time and block velocity perturbation. This can be expressed in vector and matrix form, and if the number of residual measurements exceeds the number of blocks in the model standard techniques can be used to invert for the vector of block velocity adjustments.

"Introduction To Seismology" by P. Shearer, Cambridge University Press

USGS science for a changing world

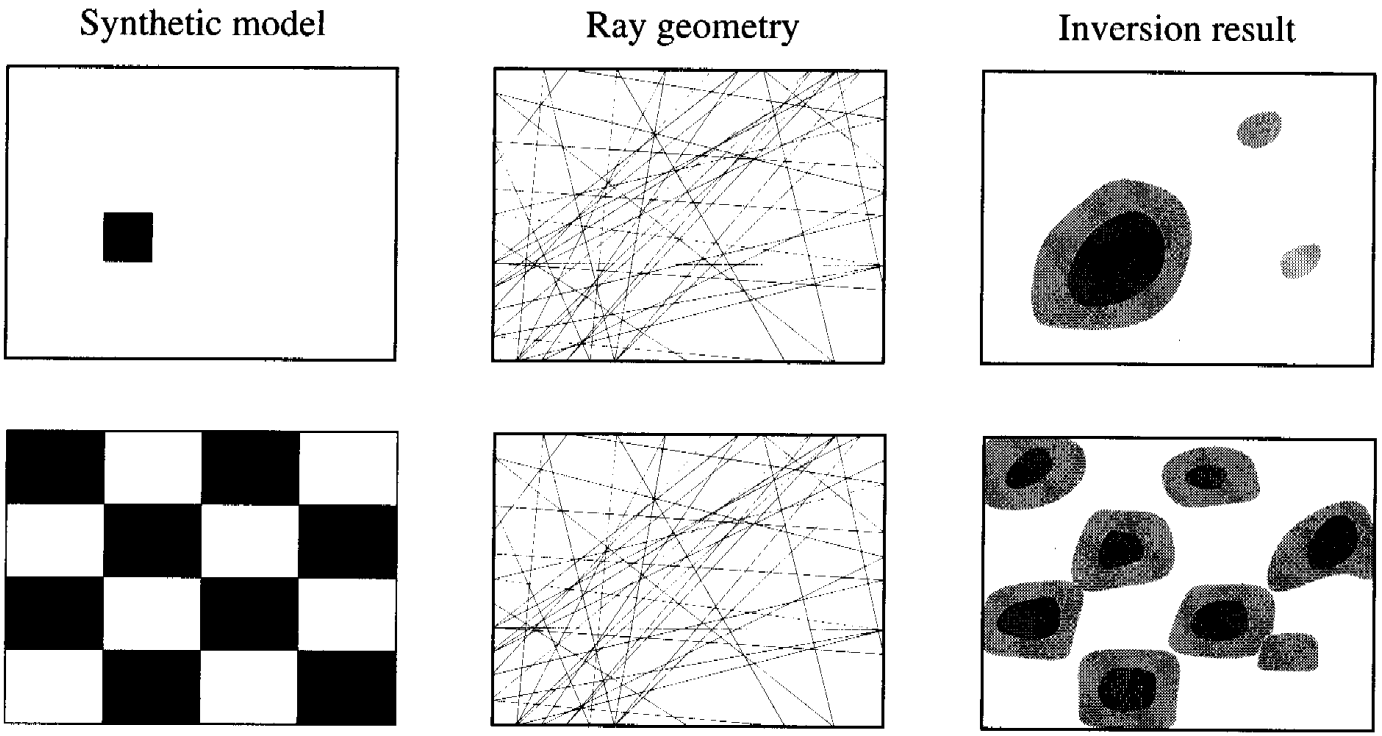

Fig. 5.7. The resolution of tomographic models is often evaluated using the impulse response test (top) or the checkerboard test (bottom). In each, a synthetic set of travel times are created for a simple velocity model using the same ray paths present in the real data; then the synthetic times are inverted to see how well the starting model is recovered.

Earthquake Location

- Earthquakes are defined by their origin time and hypocenter (location of first energy release). Inverting travel-time data for these parameters is one of the oldest challenges in seismology. Travel-time is a nonlinear function of earthquake location.

- Common approaches:
  1) Iterative (linearized) inversion methods
  2) Master event methods

CHAPTER 6

Ray Theory: Amplitude and Phase

Up to this point we have considered only the travel times of rays traveling in Earth, ignoring the amplitude, polarity, and shape of the pulses. Such an analysis is not without its merits in examining real data, since observed travel times are usually more robust and stable than amplitudes. However, amplitude and waveform shape are also important and contain valuable additional information about Earth structure and seismic sources.

To model amplitude variations, ray theory must account for geometrical spreading effects, reflection and transmission coefficients at interfaces, and intrinsic attenuation. We have already seen some aspects of geometrical spreading in the $1/r$ factor in the equations for the spherical wavefront (Section 3.5) and in the eikonal equation (Appendix 3). However, because geometrical spreading is most easily understood in terms of the energy density contained in wavefronts, we begin by examining the energy in seismic waves.

6.1 Energy in Seismic Waves

The energy density $\tilde{E}$ contained in a seismic wave may be expressed as a sum of kinetic energy $\tilde{E}_K$ and potential energy $\tilde{E}_W$:

$$\tilde{E} = \tilde{E}_K + \tilde{E}_W. \tag{6.1}$$

The kinetic energy density is given by

$$\tilde{E}_K = \tfrac{1}{2}\rho\dot{u}^2, \tag{6.2}$$

where ρ is the density and $\dot{u}$ is the velocity. This is analogous to $E = \frac{1}{2}mv^2$ from elementary physics. The potential energy density $\tilde{E}_W$ is also called *strain energy* and results from the distortion of the material (the strain) working against a restoring force (the stress). From thermodynamic considerations (e.g., see pp. 22–23 of Aki and Richards) it can be shown that

$$\tilde{E}_W = \tfrac{1}{2}\tau_{ij}e_{ij}, \tag{6.3}$$

where τ_{ij} and e_{ij} are the stress and strain tensors respectively.

To model amplitudes in ray theory we must account for geometrical spreading, reflection and transmission at interfaces, and anelastic attenuation.

Energy in a plane wave is proportional to the squares of both amplitude and frequency.

"Introduction To Seismology" by P. Shearer, Cambridge University Press

USGS science for a changing world

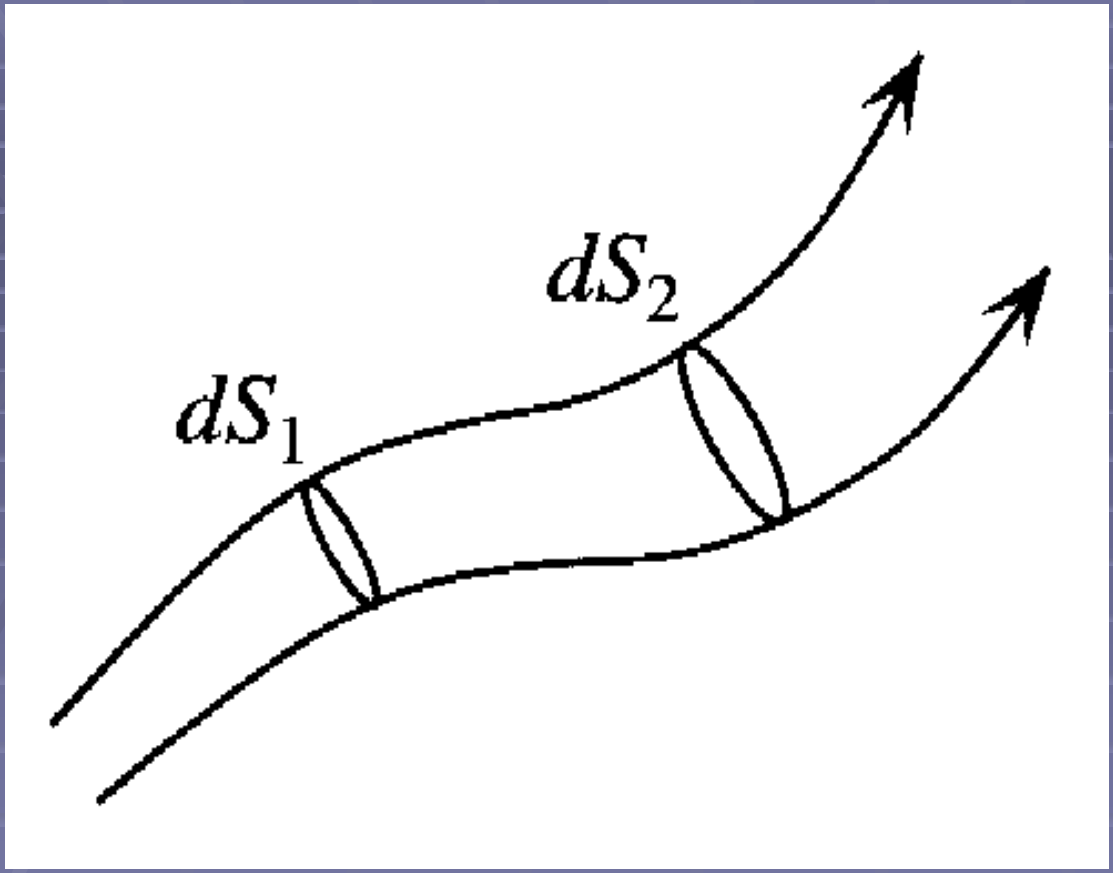

To account for geometrical effects of propagation consider a ray tube in which energy flux is conserved. As the wavefront spreads out from the source, amplitude varies inversely as the square root of the surface area of the patch enclosed by the ray tube. For a simple spherical wave the surface area grows as r^2 (r is distance) and amplitude scales as 1/r. Amplitude can actually increase if the wave is focused during propagation.

"Introduction To Seismology" by P. Shearer, Cambridge University Press

USGS science for a changing world

Figure 4.36. Waves generated at an interface between two elastic media by an incident P-wave. The incident P-wave has amplitude A_0 and angle of incidence i The reflected P- and SV-waves have angles of reflection e_1 and f_1 and amplitudes A_1 and B_1, respectively. The transmitted P- and SV-waves have angles of refraction e_2 and f_2 and amplitudes A_2 and B_2, respectively.

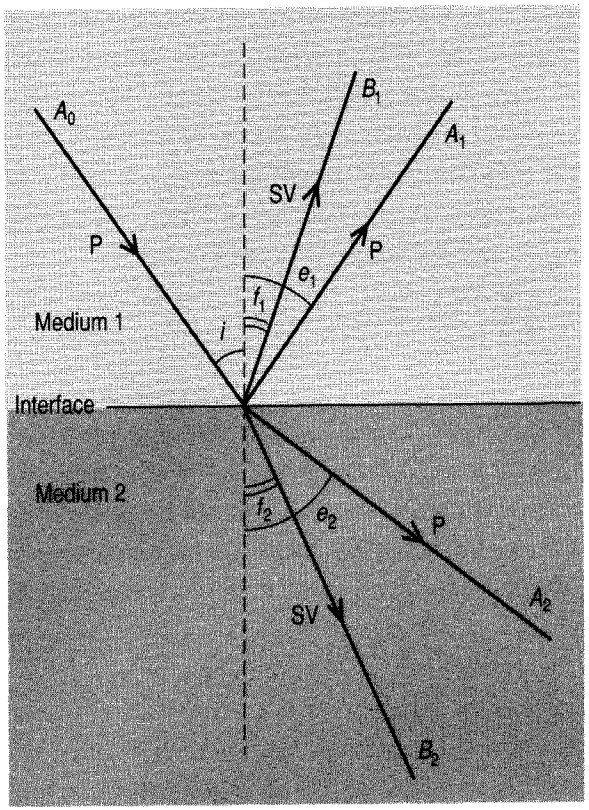

Ray paths of waves generated (reflected and transmitted) by a P-wave incident (upper left) on an interface between two media with different elastic properties.

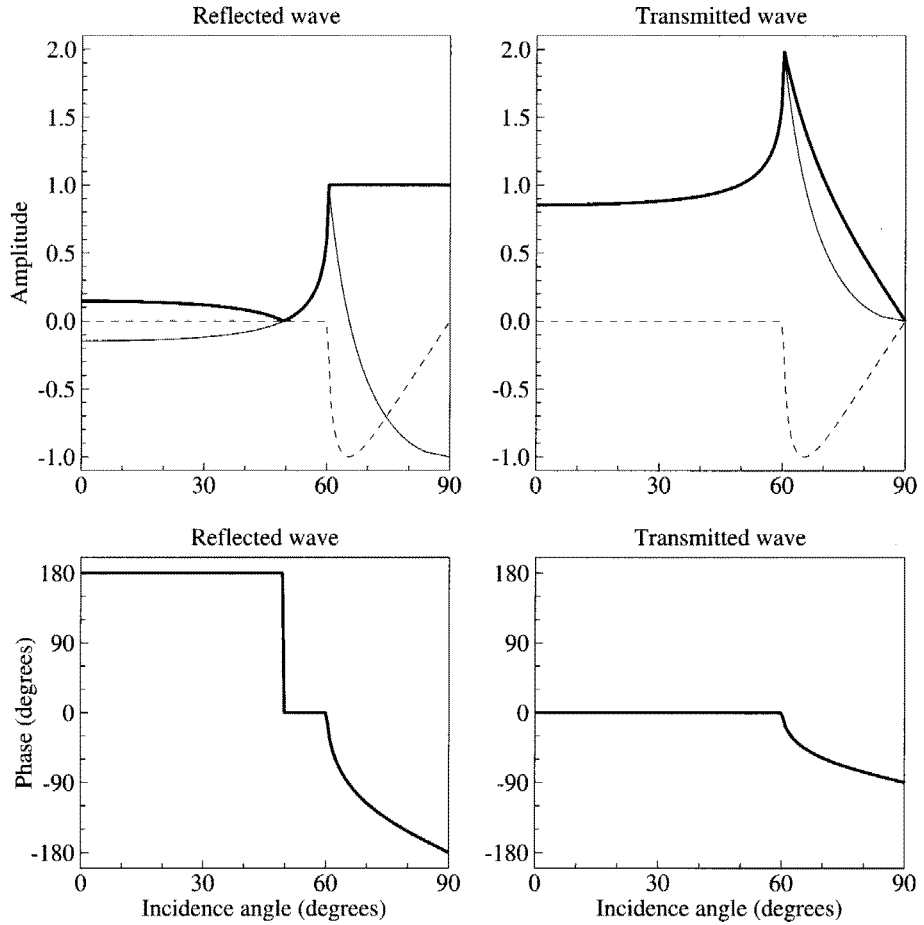

Fig. 6.4. Reflection and transmission coefficients versus ray angle for a downgoing *SH*-wave incident on the Moho. In the top plots, the real part of the reflection coefficient is shown with a thin solid line, the imaginary part with a dashed line, and the magnitude with a heavy line. The lower plots show the change in the phase angle for a harmonic wave. The sign of the imaginary part of the reflection coefficients plotted here assumes that a phase shift of $-90°$ represents a $\pi/2$ phase advance (see text).

Amplitude and phase of reflected and transmitted waves from SH-wave incident on interface as a function of incidence angle.

Modeling Plane Waves in Layers

Some problems in wave propagation are better addressed by considering plane waves instead of rays, for example the amplification of ground motion due to resonance within a near-surface layer. Powerful techniques have been developed for modeling plane-wave propagation in earth models consisting of horizontal layers. Solutions of the seismic wave equation follow from matching displacements and stresses across layer boundaries (Thomson-Haskell and reflectivity methods).

Attenuation

- In addition to geometrical spreading, seismic waves lose energy due to scattering and anelasticity as they propagate.
- Anelasticity is sometimes called internal friction since seismic energy is converted to heat.
- Energy-dissipation mechanisms include grain-boundary, grain-defect, and fluid interactions induced by dynamic stresses as seismic waves pass by.
- These processes are difficult to quantify since they must be isolated from other complex source and wave-propagation phenomena.

USGS
science for a changing world

- Attenuation is defined as the fractional energy loss per cycle of motion, and is quantified by the parameter 1/Q.
- The amplitude of a seismic wave can be written as a product of a real exponential term describing the amplitude decay from attenuation and an imaginary exponential term describing the oscillations.

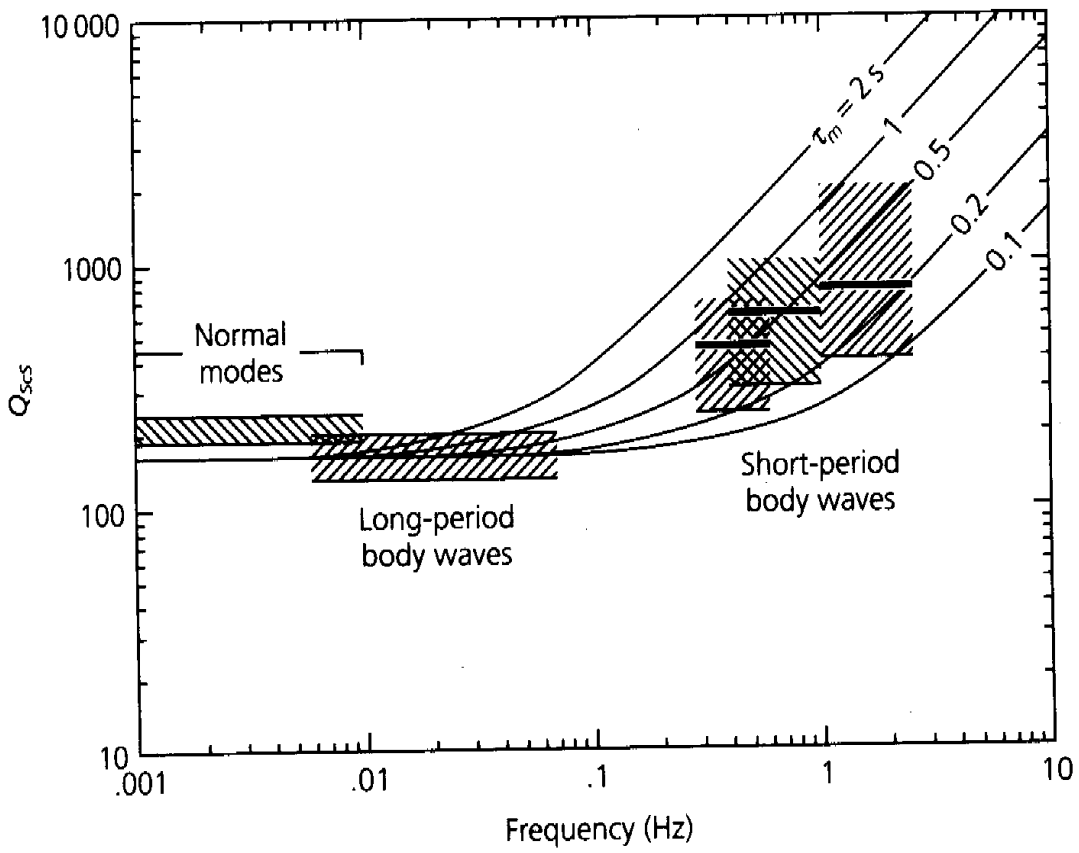

Fig. 3.7-12 Frequency dependence of attenuation for seismic waves in the mantle. Q is shown as though all measurements were for *ScS* waves, a good measure of the average mantle value because of their path from surface to core and back. (Sipkin and Jordan, 1979. © Seismological Society of America. All rights reserved.)

CHAPTER 7

Reflection Seismology

One of the most important applications of seismology involves the probing of Earth's internal structure by examining energy reflected at steep incidence angles from subsurface layers. This technique may loosely be termed *reflection seismology* and has been used extensively by the mining and petroleum industries to study the shallow crust, generally using portable instruments and artificial sources. However, similar methods can be applied to the deeper Earth using recordings of earthquakes or large explosions. Because reflected seismic waves are sensitive to sharp changes in velocity or density, reflection seismology can often provide much greater lateral and vertical resolution than can be obtained from study of direct seismic phases such as P and S (analyses of these arrivals may be termed *refraction seismology*). However, mapping of reflected phases into reflector depths requires knowledge of the average background seismic velocity structure, to which typical reflection seismic data are typically only weakly sensitive. Thus refraction experiments are a useful complement to reflection experiments when independent constraints on the velocity structure (e.g., from borehole logs) are unavailable.

Reflection seismic experiments are typically characterized by large numbers of sources and receivers at closely spaced and regular intervals. Because the data volume generally makes formal inversions too costly for routine processing, more practical approximate methods have been widely developed to analyze the results. Simple time versus distance plots of the data can produce crude images of the subsurface reflectors; these images become increasingly accurate as additional processing steps are applied to the data.

Our discussion in this chapter will be limited to P-wave reflections, as the sources and receivers in most reflection seismic experiments are designed to produce and record P-waves. Our focus will also mainly be concerned with the travel time rather than the amplitude of seismic reflections. Although amplitudes are sometimes studied, historically amplitude information has assumed secondary importance in reflection processing. Indeed often amplitudes are self-scaled prior to plotting using *automatic gain control* (AGC) techniques. Finally, we will consider a two-dimensional geometry, for which the sources, receivers and reflectors are assumed to lie within a vertical plane. Recently, an increasing number of reflection surveys involve a grid of sources and receivers on the surface that are capable of resolving three-dimensional Earth structure. Most of the concepts described in this chapter, such as common midpoint stacking and migration, are

Traditionally, reflection seismic methods were developed to explore for petroleum or mineral resources in the shallow crust. Repeatable, artificial seismic sources (explosions or vibrations) and arrays of seismometers are deployed at the earth's surface, and computer-intensive processing methods are used to map boundaries at depth. Extensive data redundancy is used to suppress noise and enhance the subsurface images.

"Introduction To Seismology" by P. Shearer, Cambridge University Press

USGS science for a changing world

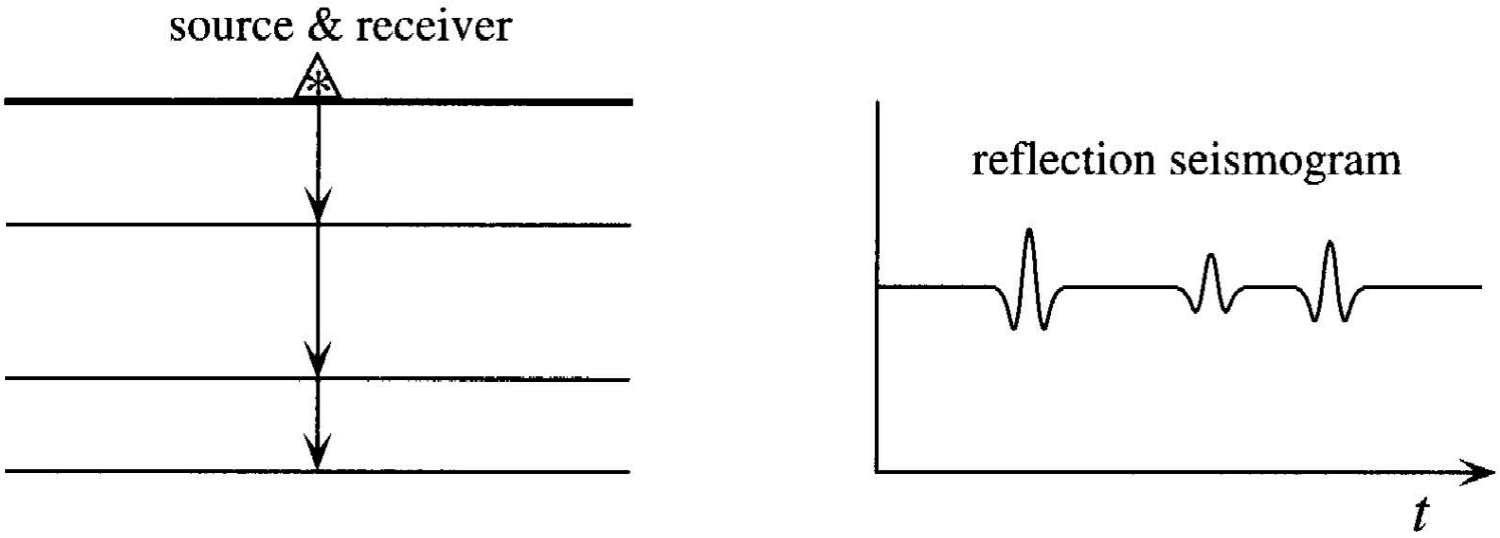

Fig. 7.1. Downgoing seismic waves from a surface source are reflected by subsurface layers, producing a seismogram with discrete pulses for each layer. In this example, the velocity contrasts at the interfaces are assumed to be small enough that multiple reflections can be ignored.

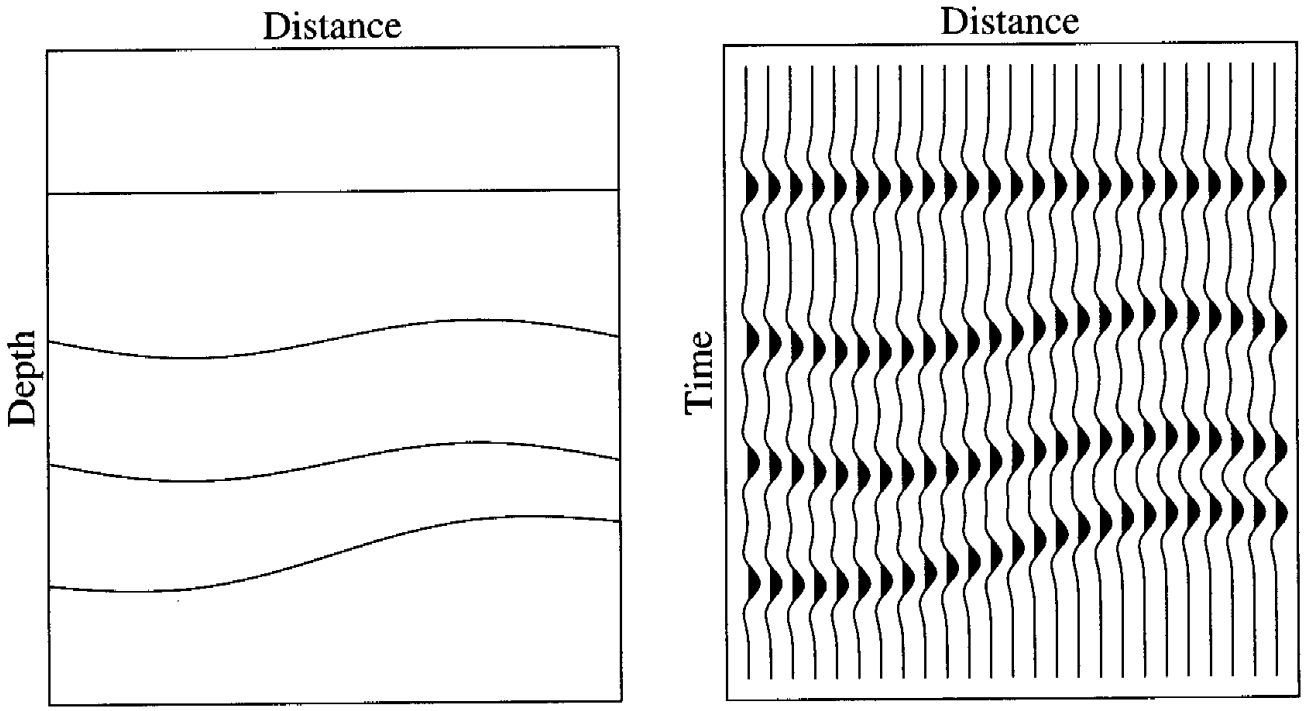

Fig. 7.2. The structural cross section on the left is imaged by an idealized zero-offset seismic reflection profile on the right. Here we have assumed that velocity is approximately constant throughout the model (except for thin reflecting layers) so that time and velocity scale linearly.

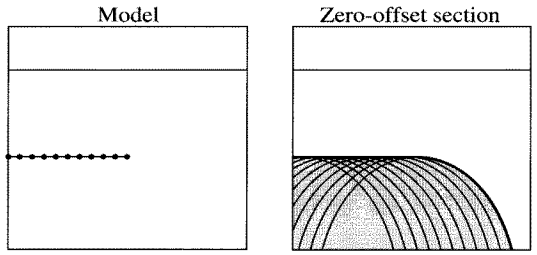

Fig. 7.10. The endpoint of a horizontal reflector will produce a diffracted arrival in a zero-offset section. The reflector itself can be modeled as the coherent sum of the diffraction hyperbola from individual point scatterers. The diffracted phase, shown as the curved heavy line, occurs at the boundary of the region of scattered arrivals.

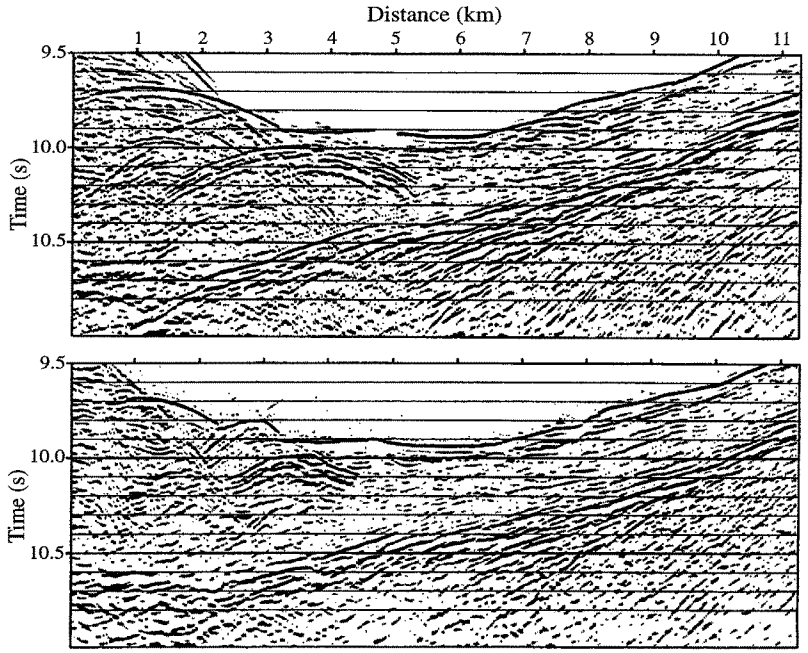

Fig. 7.11. Original (top) and migrated (bottom) reflection data from a survey line across the Japan trench (figure modified from Claerbout, 1985; data from the Tokyo University Oceanographic Research Institute).

CHAPTER 8

Surface Waves

Our treatment to this point has been limited to body waves, solutions to the seismic wave equation that exist in whole spaces. However, when free surfaces exist in a medium, other solutions are possible and are given the name *surface waves*. There are two types of surface waves that propagate along Earth's surface, *Rayleigh waves* and *Love waves*. For laterally homogeneous models, Rayleigh waves are radially polarized (P/SV) and exist at any free surface, whereas Love waves are transversely polarized and require some velocity increase with depth (or a spherical geometry). Surface waves are generally the strongest arrivals recorded at teleseismic distances and they provide some of the best constraints on Earth's shallow structure and low-frequency source properties. They differ from body waves in many respects—they travel more slowly, their amplitude decay with range is generally much less, and their velocities are strongly frequency dependent.

8.1 Love Waves

Love waves are formed through the constructive interference of high order *SH* surface multiples (i.e., *SSS*, *SSSS*, *SSSSS*, etc.). Thus, it is possible to model Love waves as a sum of body waves. To see this, consider monochromatic plane wave propagation for the case of a vertical velocity gradient in a laterally homogeneous model, a situation we previously examined in Section 6.4. In this case, a plane wave defined by ray parameter p will turn at the depth where $\beta = 1/p$. Along the surface the plane wave will propagate with horizontal slowness defined by p. If the surface bouncepoints are separated by a distance $X(t)$, then the travel time along the surface between bouncepoints is given by $pX(p)$. This follows from our definition of a plane wave and does not depend upon the velocity model.

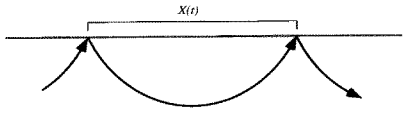

In contrast, the travel time along the ray paths is given by $T(p)$ and is a function of the velocity–depth profile.

Because these travel times are not the same, destructive interference will occur except at certain fixed frequencies. Along the surface, the phase (0 to 2π) of a

Rayleigh waves are radially polarized waves that propagate at the free surface of an elastic medium. Love waves are transversely polarized waves that require a vertical velocity gradient (or spherical geometry). Surface waves are generally the strongest arrivals at great distances from earthquakes. Compared to P and S body waves they travel more slowly, decay much less with distance, and their velocities depend strongly on frequency.

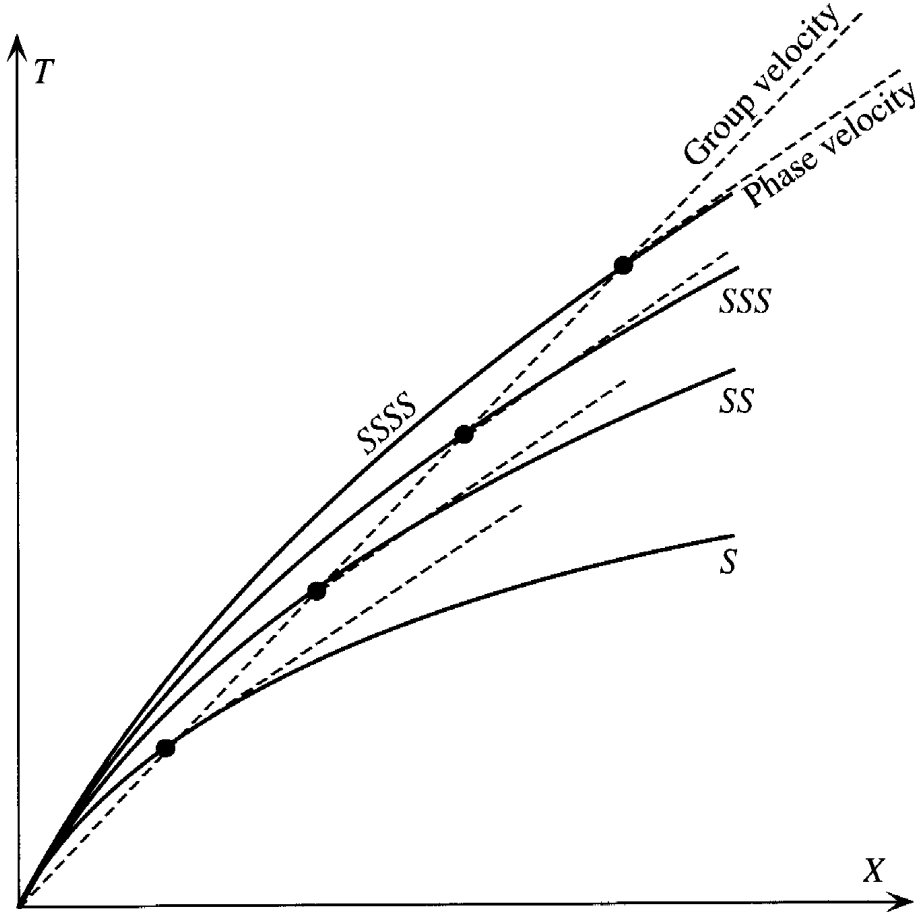

Fig. 8.1. Love waves can be constructed as a sum of S surface multiples. The dashed lines show the group and phase velocities at a fixed value of the ray parameter p; the phase velocity is faster than the group velocity.

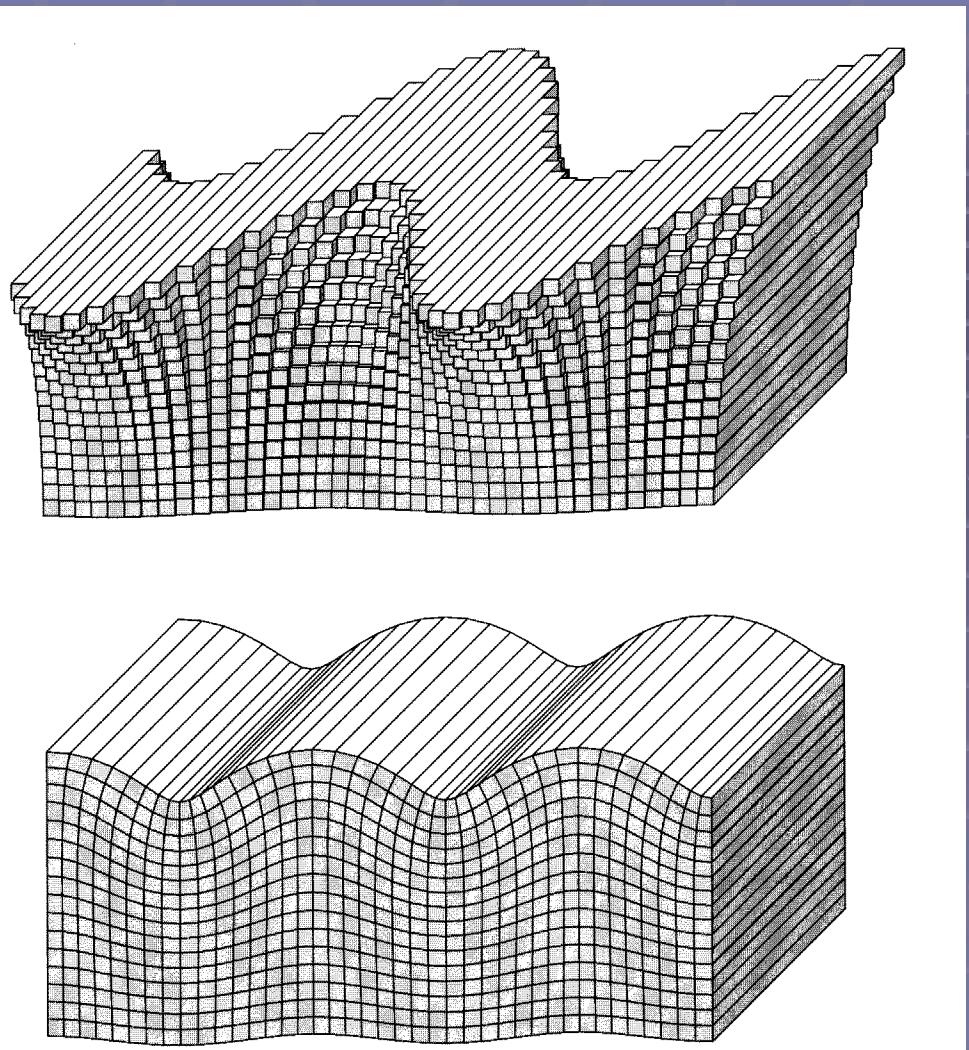

Fig. 8.4. Fundamental Love (top) and Rayleigh (bottom) surface wave displacements for horizontal propagation across the page. Love waves are purely transverse motion, whereas Rayleigh waves contain both vertical and radial motion. In both cases, the wave amplitude decays strongly with depth.

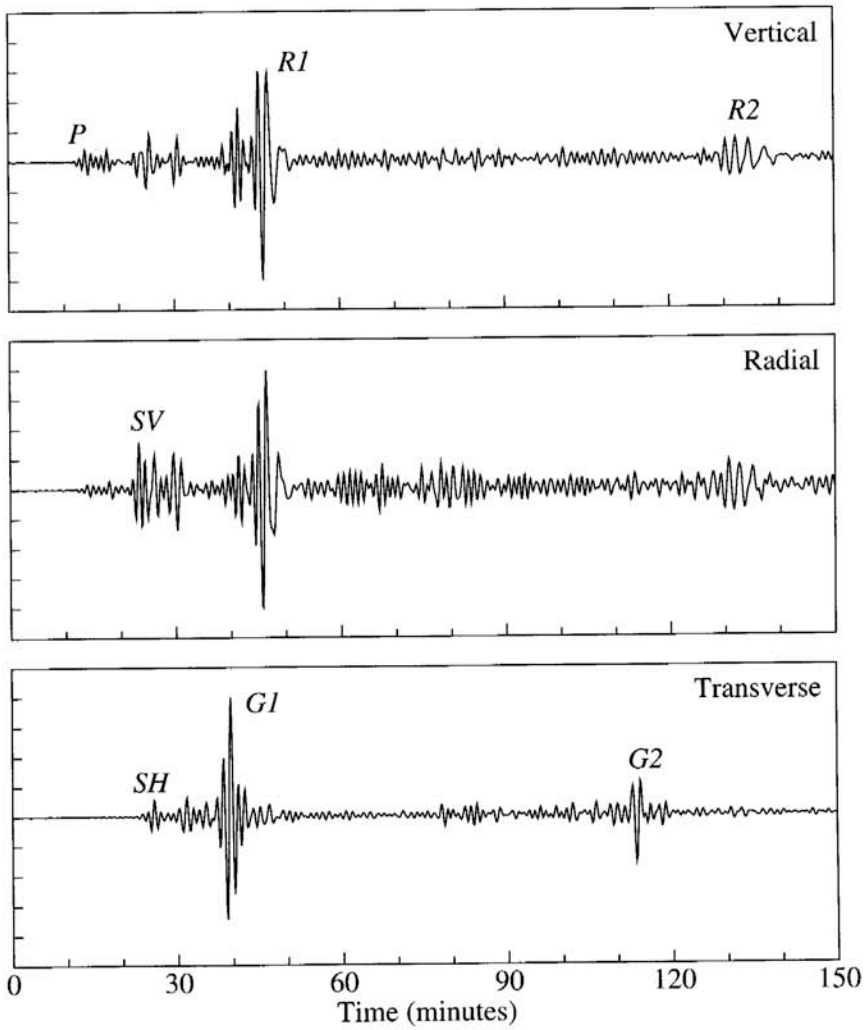

Fig. 8.8. The vertical, radial, and transverse components of motion for a March 11, 1989, earthquake at 230 km depth in the Tonga trench recorded at IRIS/IDA station NNA in Peru. *P*, *SV*, and Rayleigh waves are most visible on the vertical and radial components; *SH* and Love waves appear on the transverse component.

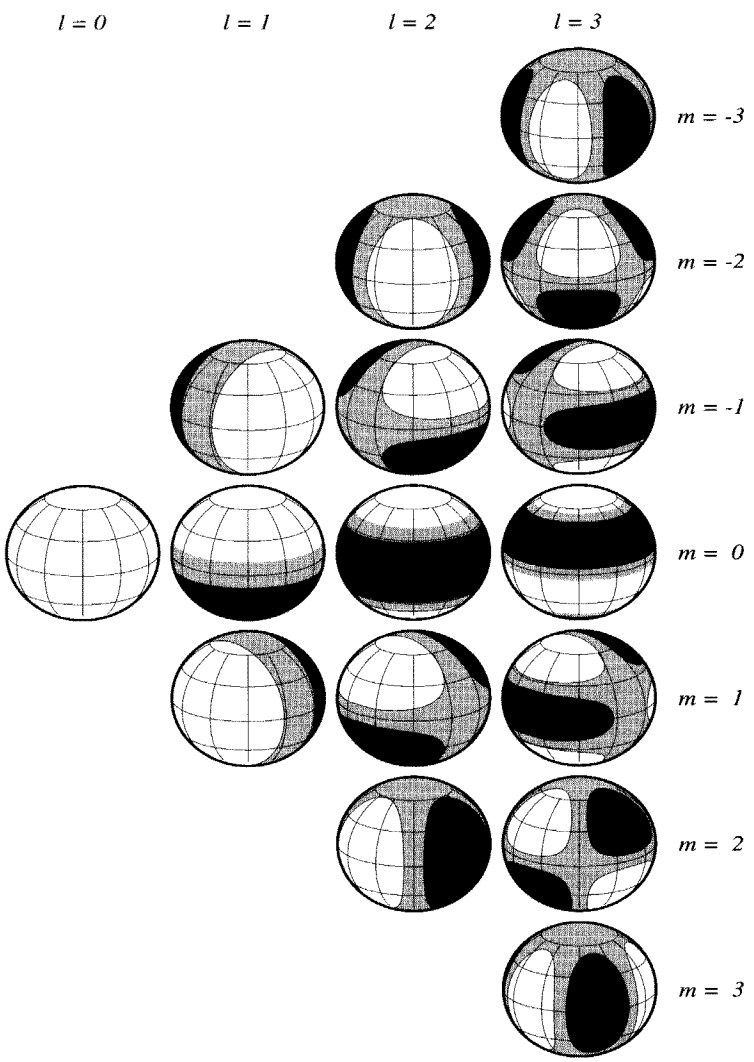

Fig. 8.11. Spherical harmonic functions Y_l^m up to degree $l = 3$. Positive values are shown as white, negative as black, with near-zero values as gray. There are $2l+1$ values of m at each degree. Note that the negative m harmonics are rotated versions of the positive m harmonics.

Earth's free oscillations can be derived as a sum of surface waves.

"Introduction To Seismology" by P. Shearer, Cambridge University Press

USGS science for a changing world

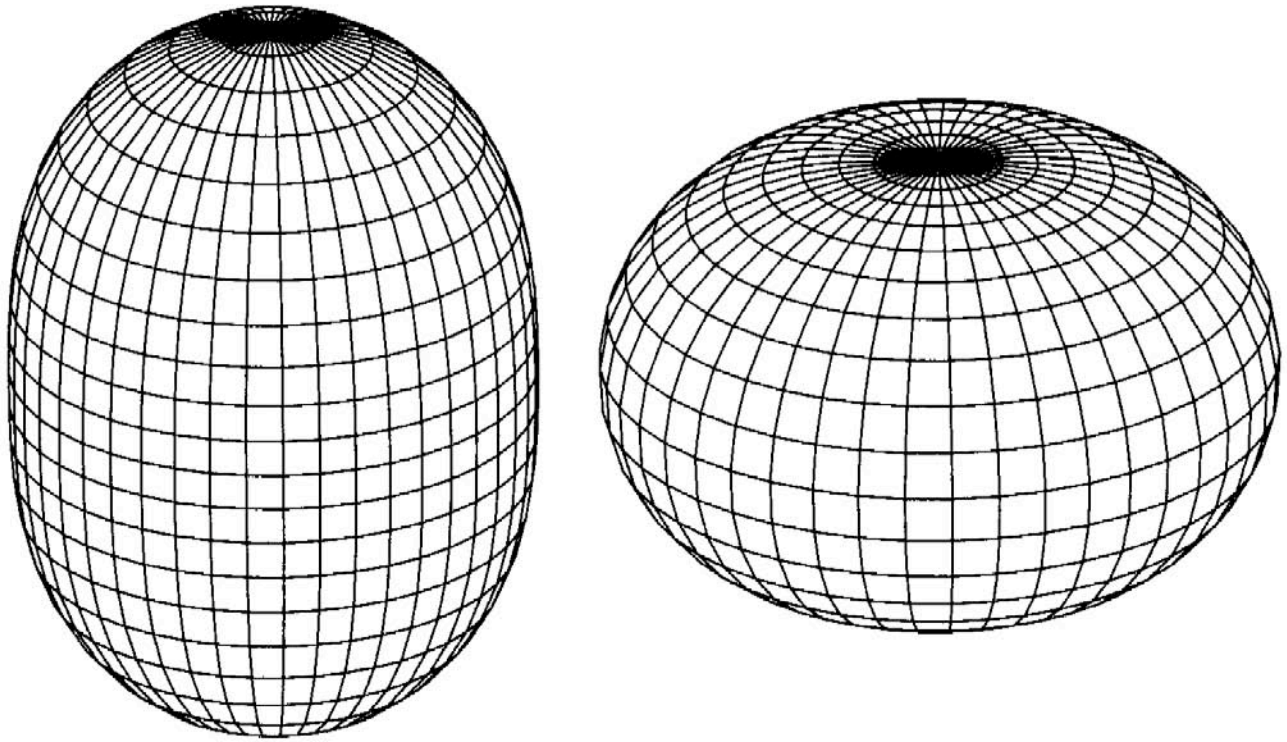

Fig. 8.12. A highly exaggerated picture of the normal mode ${}_0S_2$. This mode has a period of about 54 minutes; the two images are separated in time by 27 minutes.

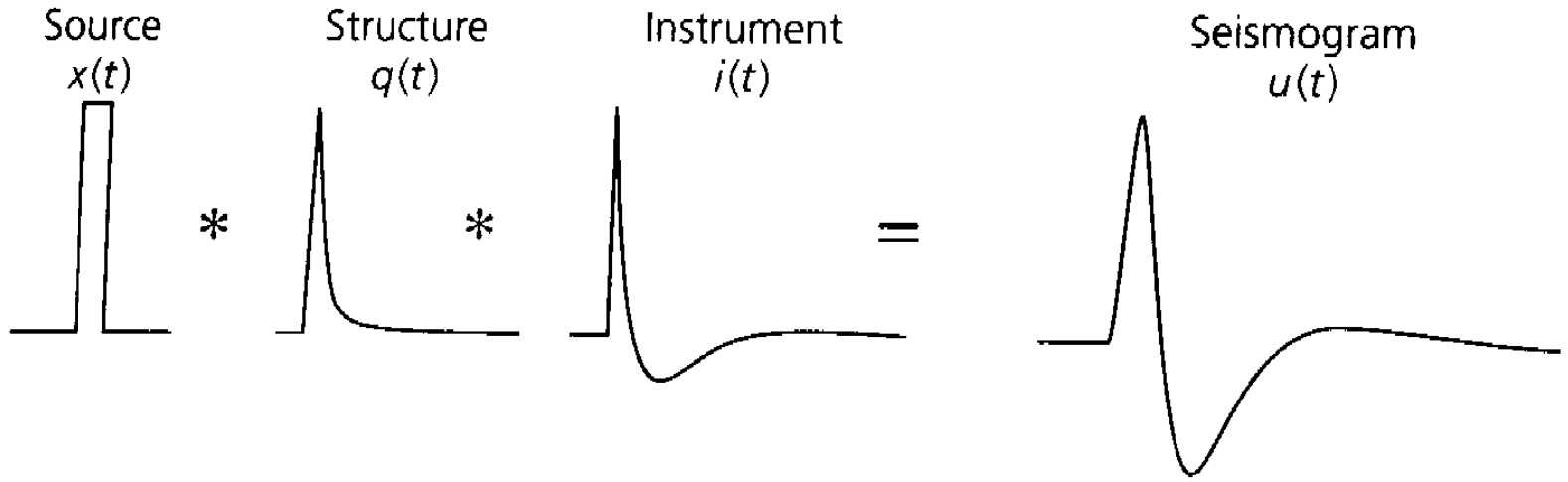

Fig. 4.3-5 The *P*-wave arrival waveform for a deep earthquake combines the effect of the source time function, attenuation, and the instrument.

To fully describe the earthquake ground shaking, we must also consider the seismic source.

CHAPTER 9

Source Theory

In the preceding chapters we have described methods for modeling the propagation of seismic waves, but we have largely neglected the question of where the waves come from and how the radiated seismic energy relates to the physical properties of the source. These topics can often be ignored if our interest is solely in learning about details of Earth structure outside of the source regions, such as travel time studies of velocity structure. However, in many cases resolving seismic structure requires some knowledge of the source characteristics, and, of course, resolving source properties is fundamental to any real understanding of earthquakes. Because seismic source theory can be very complex, we will not formally derive most of the equations in this chapter; instead we will summarize many of the important results that are of practical use in seismology and refer the reader to Aki and Richards for a more detailed theoretical treatment.

9.1 Green's Functions and the Moment Tensor

Our goal in this chapter is to understand how the observed seismic displacements at some distance from a seismic event can be related to the source properties. Let us begin by recalling the momentum equation for an elastic continuum

$$\rho \frac{\partial^2 u_i}{\partial t^2} = \partial_j \tau_{ij} + f_i, \tag{9.1}$$

where ρ is the density, u_i is the displacement, τ_{ij} is the stress tensor, and f_i is the body force term. Now consider the displacement field in a volume V bounded by a surface S. The displacements within V must be a function solely of the initial conditions, the internal forces within V, and the tractions acting on S. A more formal statement of this fact is termed the *uniqueness theorem* and is derived in Section 2.3 of Aki and Richards. It turns out that specifying either the tractions or the displacement field on S, together with the body forces $\mathbf{f}$, is sufficient to uniquely determine $\mathbf{u}$ throughout V.

Solving (9.1) in general is quite difficult if we include the f_i term, and in Chapter 3 we quickly dropped it to concentrate on the homogeneous equation of motion. Let us now explore how the properties of the source can be modeled and related to the seismic displacements observed in the Earth. Consider a unit force vector $\mathbf{f}(\mathbf{x}_0, t_0)$ applied at point $\mathbf{x}_0$ at time t_0. By itself, this is not a realistic seismic source; rather, it is what would result if the hand of God could reach

Slip on a fault can be modeled as a distribution of idealized simple forces that produces exactly the same displacement field as the slip.

"Introduction To Seismology" by P. Shearer, Cambridge University Press

USGS science for a changing world

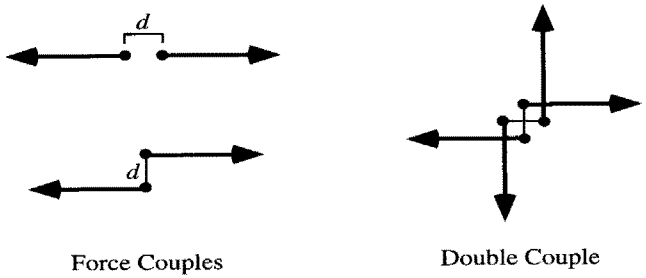

Fig. 9.1. Force couples are opposing point forces separated by a small distance. A double couple is a pair of complementary couples that produce no net torque.

We define the force couple M_{ij} in a Cartesian coordinate system as a pair of opposing forces pointing in the i direction, separated in the j direction. The nine different force couples are shown† in Figure 9.2. The magnitude of M_{ij} is given by the product fd and is assumed constant as d goes to zero in the limit of a point source. It is then natural to define the *moment tensor* $\mathbf{M}$ as

$$\mathbf{M} = \begin{bmatrix} M_{11} & M_{12} & M_{13} \\ M_{21} & M_{22} & M_{23} \\ M_{31} & M_{32} & M_{33} \end{bmatrix}. \qquad (9.3)$$

To conserve momentum, internal forces must be specified as balanced force couples. If we can compute the ground motion from a single idealized force (the Green's function) the full seismic wave field can be computed as a linear superposition. The strength of the force is given by the seismic moment, the product of the shear modulus of the source medium, the slip displacement on the fault, and the fault area.

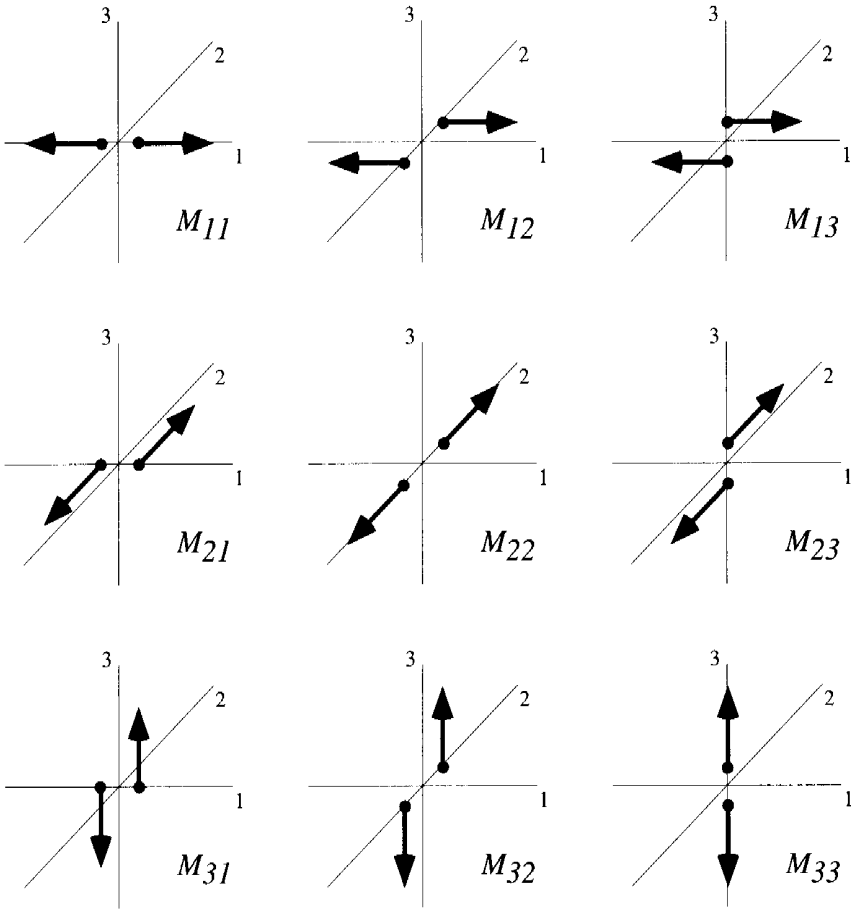

Fig. 9.2. The nine different force couples that make up the components of the moment tensor.

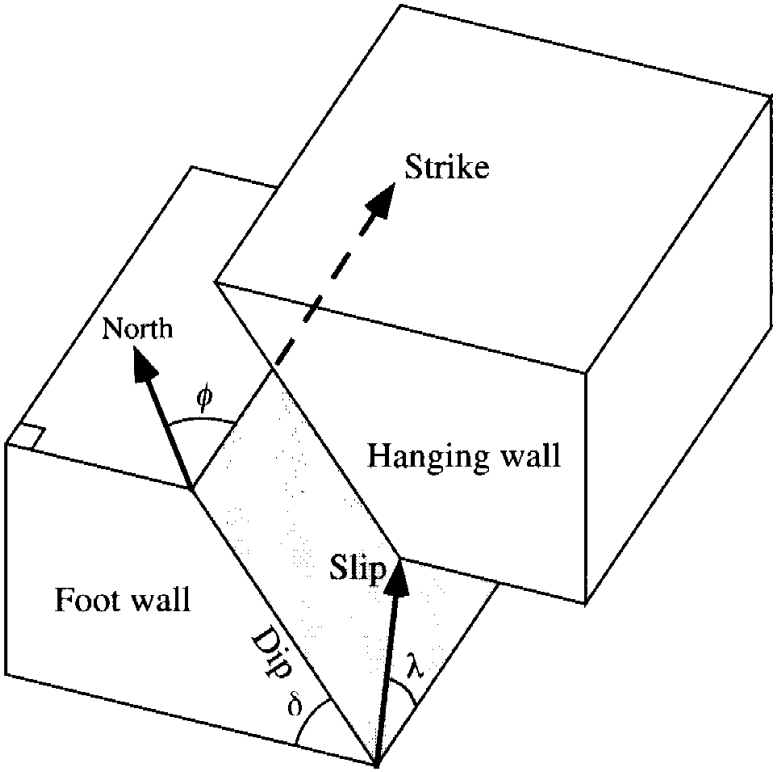

Fig. 9.3. A planar fault is defined by the strike and dip of the fault surface and the direction of the slip vector.

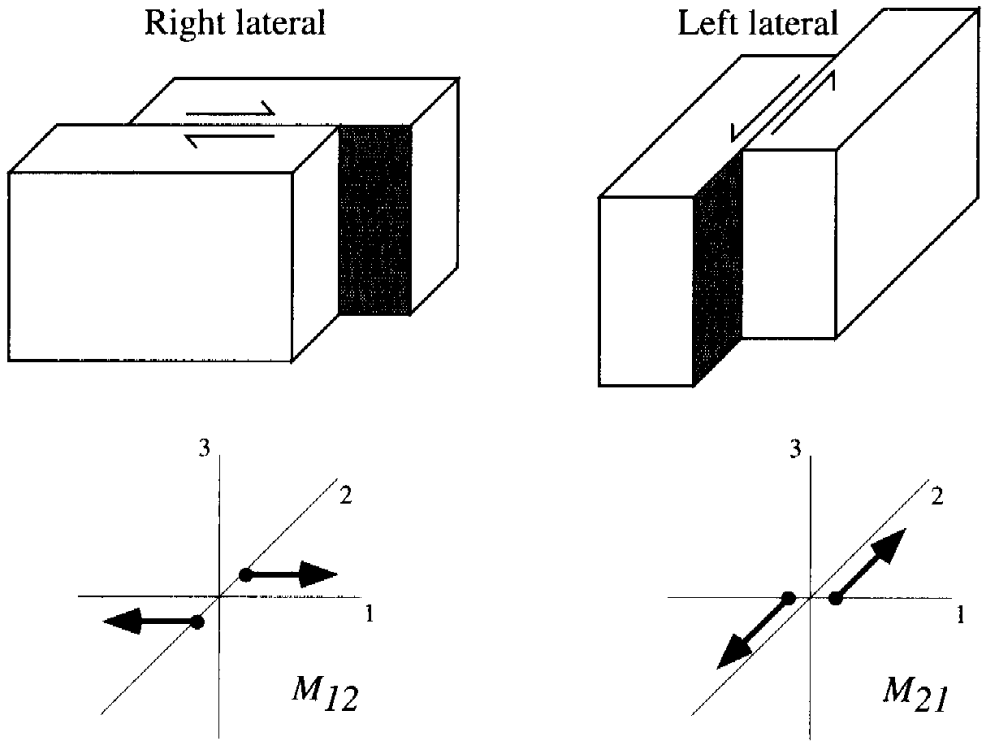

Fig. 9.4. Owing to the symmetry of the moment tensor, these right-lateral and left-lateral faults have the same moment tensor represention and the same seismic radiation pattern.

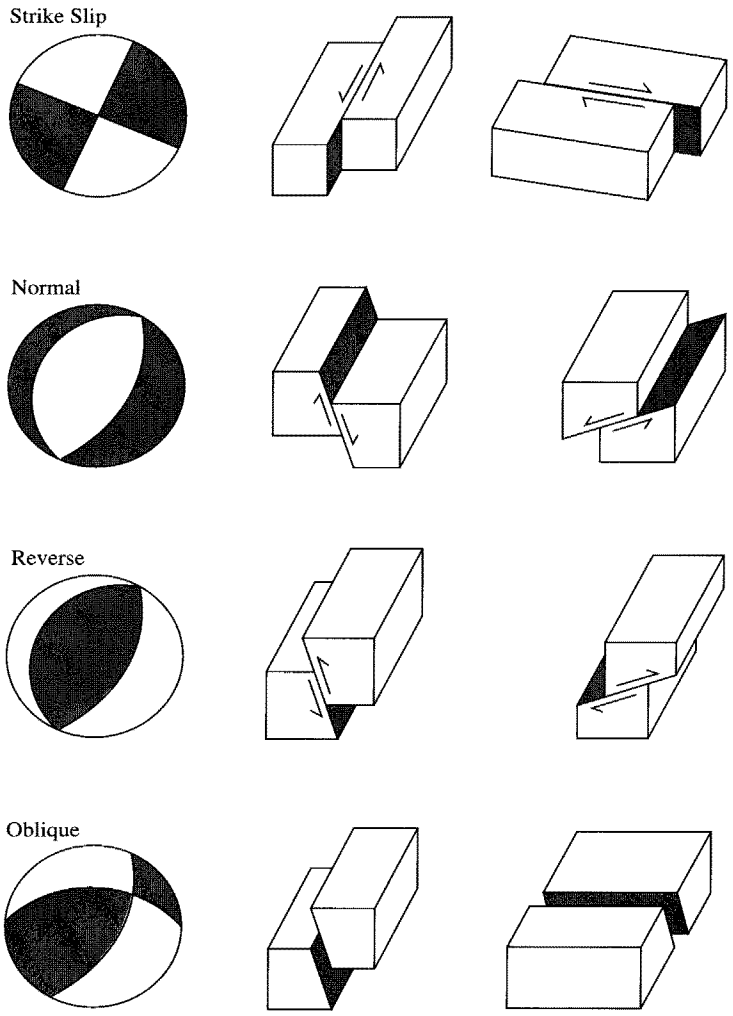

Fig. 9.8. Examples of focal spheres and their corresponding fault geometries. The lower half of the focal sphere is plotted to the left, with the compressional quadrants shaded. The block diagrams on the right show the two fault geometries (the primary and auxillary fault planes) that could have produced the observed radiation pattern.

If we generalize the concept of the scalar moment ($M_0 = \mu D A$) from Section 9.2 to be time dependent, we may define

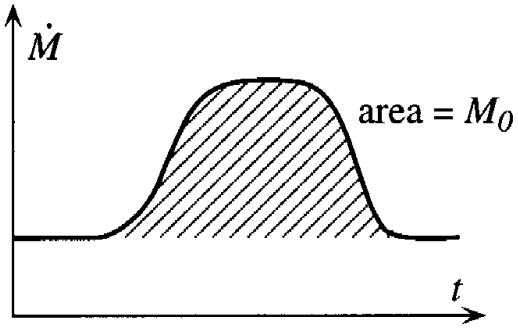

$$\dot{M}(t) = \mu \frac{\partial}{\partial t}[A(t)D(t)], \tag{9.19}$$

and the area under the $\dot{M}(t)$ function represents M_0, the total change in $M(t)$, which can be expressed as

$$M_0 = \mu \overline{D} A, \tag{9.20}$$

where μ is the shear modulus, $\overline{D}$ is the average displacement across the fault, and A is the area of the fault.

Slip across the fault is generally not instantaneous, but occurs over a finite duration. The time dependence of the source controls the amplitude and timing of seismic waves.

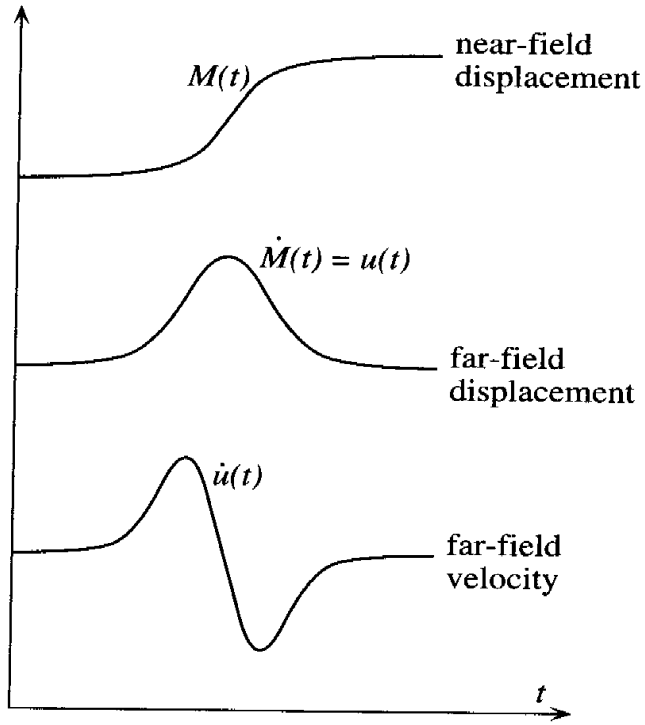

Fig. 9.10. The relationships between near-field displacement and far-field displacement and velocity.

Offsets across the fault ("near-field") are permanent, but at greater distances the wavefield is dominated by dynamic ("far-field") displacements that decay back to zero after the seismic waves pass by. The far-field displacement scales like the time derivative of the seismic moment (previous slide).

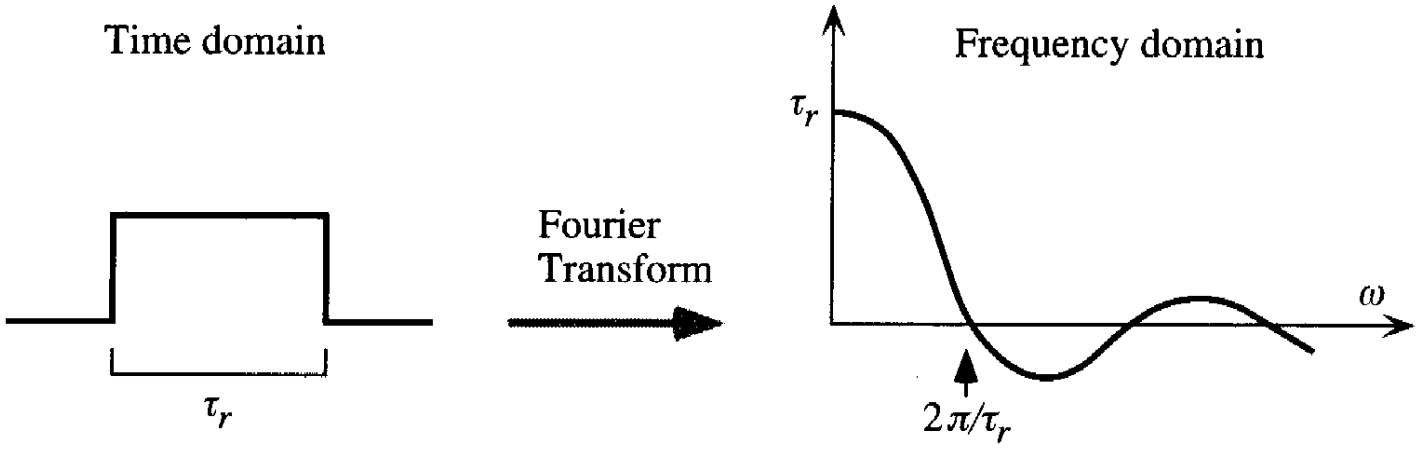

Fig. 9.14. A boxcar pulse in the time domain produces a sinc function in the frequency domain.

It is often more convenient to think about source processes in the frequency domain rather than the time domain.

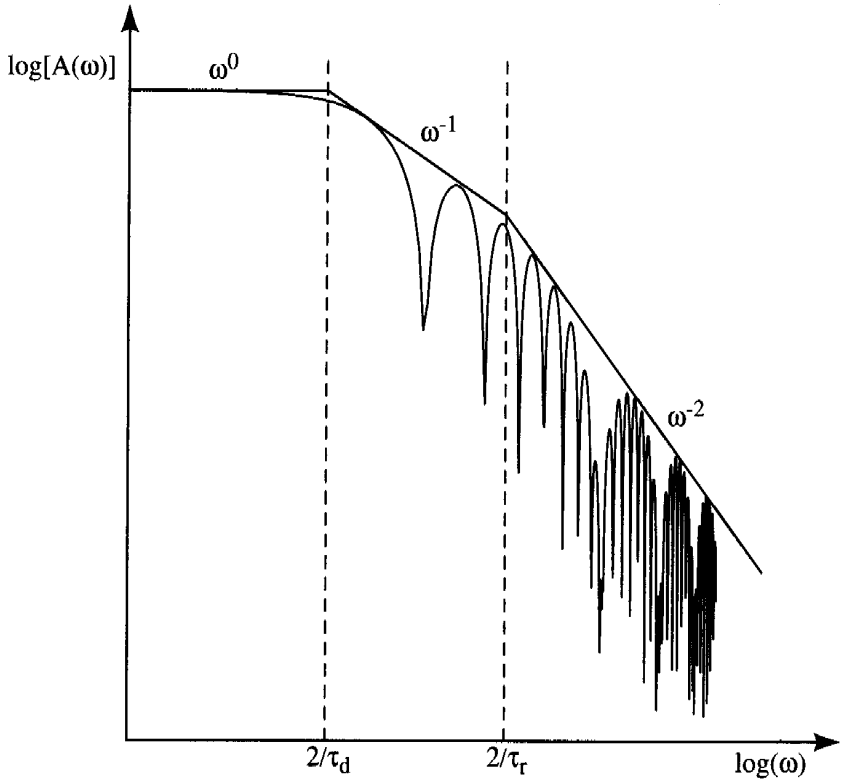

Fig. 9.15. The amplitude spectrum for the ω^{-2} source model. The spectrum is the product of two sinc functions, corresponding in the time domain to the convolution of two boxcar functions of durations τ_d and τ_r. The spectral amplitudes fall off as ω^{-1} for $2/\tau_d < \omega < 2/\tau_r$ and as ω^{-2} for $\omega > 2/\tau_r$. For the spectrum plotted in this figure, $\tau_d = 8\tau_r$.

The low-frequency level of the displacement spectrum is proportional to the seismic moment - the strength or size of the earthquake. The shape of the spectrum at higher frequencies tells us about the details of the time dependence and complexity of the slip.

"Introduction To Seismology" by P. Shearer, Cambridge University Press

USGS science for a changing world

Stress Drop

- Stress drop is defined as the average difference between stress on a fault before and after an earthquake. Released ("dropped") elastic stress is what generates permanent ground deformation and seismic waves.
- We can estimate stress drop from field measurements of average slip, fault dimension, and shear modulus.
- Alternatively, stress drop can be estimated from seismic data. Seismic moment and fault rupture dimension can be estimated from the levels and shapes of source spectra, and stress drop computed for a specific fault shape (e.g., Brune's model).

"Introduction To Seismology" by P. Shearer, Cambridge University Press

USGS science for a changing world

Source Scaling and Magnitude

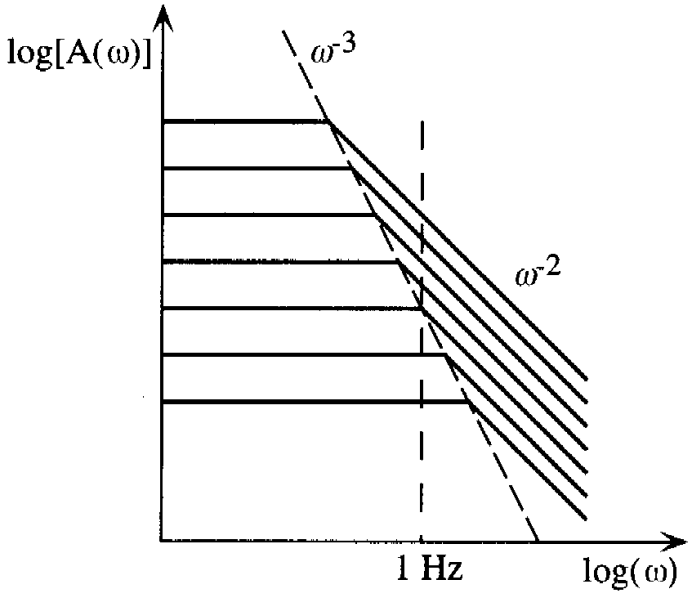

Fig. 9.17. For larger events, the corner in the source spectrum moves to lower frequencies, reducing the observed amplitude at a fixed frequency point.

Traditional magnitudes are measured at specific ground motion frequencies. These idealized source spectra show how spectral level and corner frequency scale with earthquake size. Ground motion measured near 1 Hz saturates (does not continue to scale upward with seismic moment) for earthquakes larger than about magnitude 7. This leads to inconsistencies between magnitude scales and misrepresentation of the relative sizes of large earthquakes. Seismic moment and moment magnitude overcome these limitations of traditional period-based magnitude measurements.

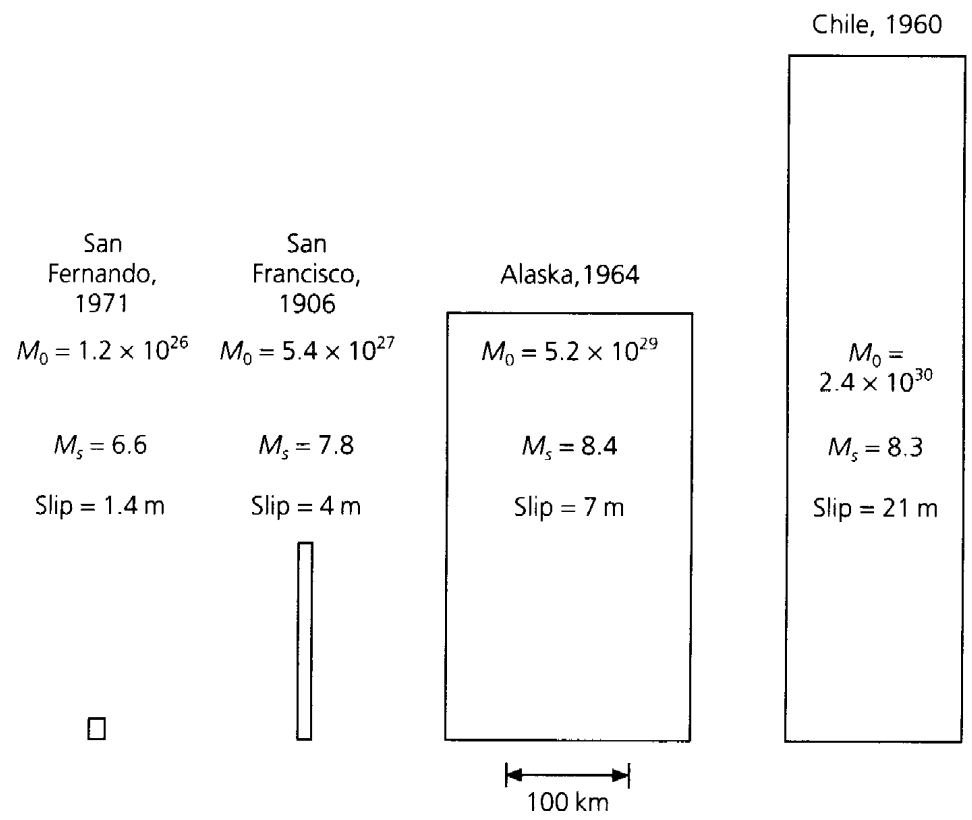

Fig. 4.6-3 Comparison of moment, magnitudes, fault area, and fault slip for four earthquakes listed in Table 4.6-1. M_s saturates for events with $M_w > 8$ and so is no longer a useful measure of earthquake size.

Table 9.1. Some Big Earthquakes (M_0 in 10^{20} N m)

Date	Region	m_b	M_S	M_w	M_0
1992 June 28	Southern California	6.2	7.3	7.5	2
1906 April 18	San Francisco		8.2	7.9	10
1989 May 23	Macquarie Ridge	6.4	8.2	8.2	20
1994 June 9	Bolivia	7.0		8.2	26
1977 August 19	Indonesia		8.1	8.3	30
1957 March 9	Aleutian Islands		8.2	9.1	585
1964 March 28	Alaska		8.4	9.2	820
1960 May 22	Chile		8.3	9.5	2000